Gondwana Research 93 (2021) 73–88

Contents lists available at ScienceDirect

Gondwana Research

journal homepage: www.elsevier.com/locate/gr

Syn-collisional detrital zircon source evolution in the northern Moroccan Variscides

Cristina Accotto [a,*], David Martínez Poyatos [a], Antonio Azor [a], Cristina Talavera [b], Noreen Joyce Evans [c], Antonio Jabaloy-Sánchez [a], Ali Azdimousa [d], Abdelfatah Tahiri [e], Hassan El Hadi [f]

[a] Departamento de Geodinámica, Universidad de Granada, Granada, Spain
[b] School of Geosciences, University of Edinburgh, Edinburgh, UK
[c] School of Earth and Planetary Science, John de Laeter Centre, Curtin University, Bentley, Australia
[d] Faculté Pluridisciplinaire de Nador et Laboratoire des Géosciences Appliquées, Faculté des Sciences, Université Mohammed I, Oujda, Morocco
[e] Laboratory of Geo-biodiversity and Natural Patrimony (GEOBIO), Scientific Institut; Geophysics, Natural Patrimony and Green Chemistry Research Center (GEOPAC), Mohammed V University in Rabat, Morocco
[f] Laboratory of Geodynamics of Ancient Belts, Faculty of Science Ben M'Sik, Hassan II, University of Casablanca, Morocco

ARTICLE INFO

Article history:
Received 13 August 2020
Received in revised form 23 December 2020
Accepted 2 February 2021
Available online 5 February 2021

Editor: S. Tappe

Keywords:
Detrital zircon provenance
Moroccan Mesetas
syn-collisional sediments
Avalonian magmatic arc

ABSTRACT

U–Pb dating and Hf isotopic analyses of detrital zircon grains from Cambrian-Devonian strata in the Moroccan Mesetas were undertaken in order to constrain its Paleozoic paleogeographic evolution. In this work, we analyzed 12 Late Devonian-Late Carboniferous samples of *syn*-collisional detrital rocks from the Western and Eastern Moroccan Mesetas. All our samples present significant Ediacaran (ca. 620 Ma) and Rhyacian (ca. 2.1 Ga) detrital zircon populations, suggesting that the West African Craton remained the main source of sediments for northern Morocco at least until the Late Carboniferous. Locally, a Stenian-Tonian (ca. 1.0 Ga) detrital zircon population is also present, probably fed from intermittent and distant source areas located in NE Africa (e.g. Sahara Metacraton). The collisional evolution started with the approach of an Avalonian promontory to the northern Gondwana continental margin (latest Devonian - earliest Carboniferous), after the closure of the Rheic Ocean. This process entailed the former subduction of the Rheic oceanic lithosphere underneath the Avalonian continental terrane and the formation of a magmatic arc in the upper plate. In this scenario, the first *syn*-collisional sediments (Tournaisian; Tiflet and Debdou-Mekkam areas) are characterized by a Devonian detrital zircon population (ca. 370 Ma), presumably derived from the magmatic arc, and an increasing number of Mesoproterozoic dates, putatively also sourced from the continental crust of the Avalonian terrane. After the initial collision, only the Visean samples located in areas close to the exotic terrane (e.g. Ben Slimane area) displayed a minor Avalonian component. Finally, the Late Carboniferous samples from the Jerada area recorded an important Middle Carboniferous (ca. 330 Ma) detrital zircon population, probably sourced from Variscan granitoids emplaced in the Eastern Moroccan Meseta and attesting to crustal thickening and subsequent thermal maturation of the Gondwana continental crust in this area.

1. Introduction

The study of syn-orogenic sediments is key to understanding collisional processes and orogenesis. In this regard, the age and distribution of syn-orogenic basins have traditionally been used to constrain the temporal and spatial evolution of the ongoing collision. Furthermore, the composition of the detrital fraction of syn-orogenic sediments can help to clarify which rocks were exhumed as a consequence of underthrusting (and/or extensional deformation) and concomitant mountain building/erosion. The possibility of dating some of the minerals included in the detrital fraction of syn-orogenic sediments has introduced a new dimension to the study of orogenesis and paleogeotectonic reconstructions. Thus, the systematic dating of minerals, especially zircon, is now used to track the continental terranes involved in collision, the successive input from originally deeper - and older - sources, and the contribution of *syn*-collisional neoformed magmatic sources.

The Late Paleozoic Variscan belt constitutes an excellent opportunity to evaluate the role of systematic syn-orogenic sediment detrital zircon dating in elucidating orogenic evolution (e.g. Pastor-Galán et al., 2013a, 2013b; Pereira et al., 2012, 2020a). This orogen resulted from Devonian-Permian complex collision between Gondwana and Laurussia, with a number of peri-Gondwanan terranes also involved in the process (e.g. Franke et al., 2017; Matte, 2001; Simancas et al., 2005). In the Moroccan

* Corresponding author.
E-mail address: accotto@ugr.es (C. Accotto).

https://doi.org/10.1016/j.gr.2021.02.001
1342-937X/

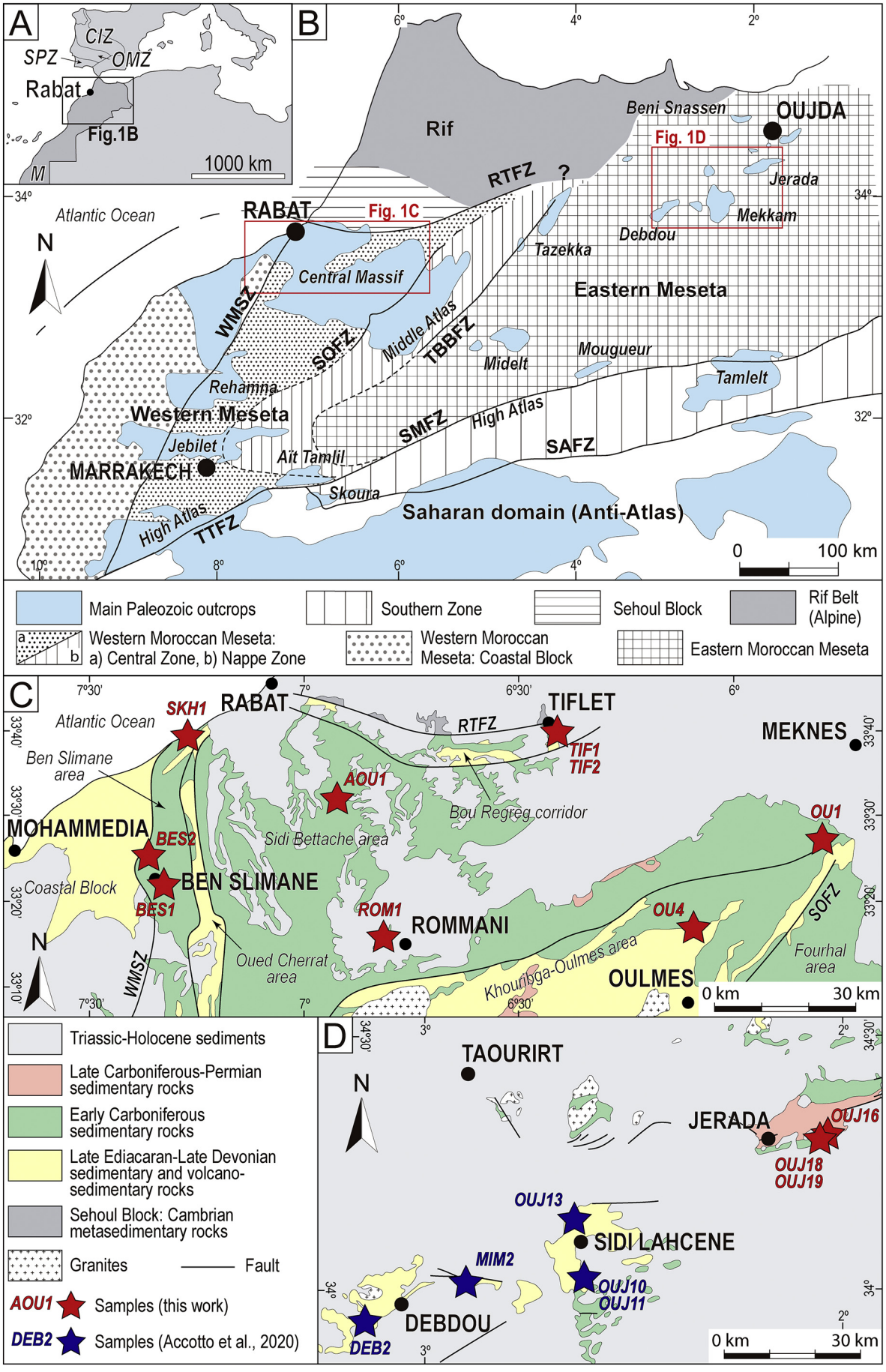
A
CIZ
SPZ
OMZ
Rabat
Fig.1B
M
1000 km
B
Rif
Beni Snassen
OUJDA
Fig. 1D
RTFZ
?
Jerada
Mekkam
Debdou
Tazekka
Eastern Meseta
Atlantic Ocean
N
RABAT
Fig. 1C
Central Massif
WMSZ
SQFZ
Middle Atlas
TBBFZ
Midelt
Mougueur
Tamlelt
Rehamna
Western Meseta
SMFZ
High Atlas
SAFZ
Jebilet
Ait Tamlil
MARRAKECH
Skoura
Saharan domain (Anti-Atlas)
High Atlas
TTFZ
0 100 km
Main Paleozoic outcrops
Southern Zone
Sehoul Block
Rif Belt (Alpine)
Western Moroccan Meseta: a) Central Zone, b) Nappe Zone
Western Moroccan Meseta: Coastal Block
Eastern Moroccan Meseta
C
Atlantic Ocean
SKH1
RABAT
RTFZ
TIFLET
TIF1
TIF2
MEKNES
Ben Slimane area
AOU1
Bou Regreg corridor
OU1
MOHAMMEDIA
BES2
Sidi Bettache area
Coastal Block
BEN SLIMANE
BES1
ROM1
ROMMANI
OU4
SQFZ
N
WMSZ
Oued Cherrat area
Khouribga-Oulmes area
Fourhal area
OULMES
0 km 30 km
Triassic-Holocene sediments
Late Carboniferous-Permian sedimentary rocks
Early Carboniferous sedimentary rocks
Late Ediacaran-Late Devonian sedimentary and volcano-sedimentary rocks
Sehoul Block: Cambrian metasedimentary rocks
Granites
Fault
AOU1 Samples (this work)
DEB2 Samples (Accotto et al., 2020)
D
TAOURIRT
N
JERADA
OUJ16
OUJ18
OUJ19
OUJ13
SIDI LAHCENE
MIM2
OUJ10
OUJ11
DEBDOU
DEB2
0 km 30 km

transects of the Variscan orogen, detrital zircon investigations have been focused on the pre-orogenic evolution (e.g. Abati et al., 2010; Accotto et al., 2019, 2020; Avigad et al., 2012; Ghienne et al., 2018; Letsch et al., 2018; Pérez-Cáceres et al., 2017), but to date, no data have been reported on the *syn*-orogenic sediments, with the exception of a recent work on the Eastern Moroccan Meseta (Accotto et al., 2020). The present work provides a wide-scale study of U–Pb geochronological and Hf isotope detrital zircon analyses carried out on syn-collisional Late Devonian-Late Carboniferous samples from the Western and Eastern Moroccan Mesetas.

2. Geological setting

The Paleozoic successions of northwestern Africa (Fig. 1A) crop out in different domains of the Moroccan Mesetas and surroundings (Fig. 1B), having been variably affected by the Variscan orogeny. These domains are separated by putative regional fault zones, the paleogeographic importance of which is unclear and controversial (e.g. Hoepffner et al., 2006; Michard et al., 2010a, 2010b; Simancas et al., 2009, 2010). The Rabat-Tiflet Fault Zone (RTFZ; Fig. 1B) separates the Moroccan Mesetas domains from the Sehoul Block, located to the north and characterized by a Cambrian siliciclastic succession affected by Caledonian penetrative deformation and intruded by Devonian granites (Michard et al., 2010b; Simancas et al., 2005; Tahiri et al., 2010). Due to this Caledonian deformation, which did not affect any other domain of the Moroccan Variscides, the Sehoul Block is considered to be part of an exotic Avalonian promontory (Simancas et al., 2005), juxtaposed to the Moroccan Mesetas during the Carboniferous. South of the RTFZ, the Western Moroccan Meseta (WMM) is divided into three subdomains, namely the Coastal Block to the west, the Central Zone, and the so-called "Nappe Zone" to the east, separated by the Western Meseta Shear Zone (WMSZ) and the Smaala-Oulmès Fault Zone (SOFM), respectively (Fig. 1B; Michard et al., 2010b). Eastwards, the Tazekka-Bsabis-Bekrit Fault Zone (TBBFZ) juxtaposes the WMM to the Eastern Moroccan Meseta (EMM). Finally, the South Meseta Fault Zone (Hoepffner et al., 2006) separates the Moroccan Mesetas from the Southern Zone, and, further south, the South Atlas and the Tizin'Test Fault Zones represent the limit of the Gondwanan foreland (Anti-Atlas; Michard et al., 2010b).

The igneous Precambrian basement of the northern Moroccan Variscides crops out in the WMM in relatively small and isolated areas of the Central Zone and Coastal Block (e.g. El Haibi et al., 2020; El Houicha et al., 2018; Ouabid et al., 2017; Pereira et al., 2014, 2015; Tahiri et al., 2010). This basement is covered by a thick, more or less continuous, passive margin succession that is exposed in large areas of the WMM, and in more scarce and relatively small inliers of the EMM (Fig. 1). The Cambrian-Silurian succession is mainly terrigenous, with the exception of local Lower Cambrian limestones in the WMM (Michard et al., 2010b and references therein); in the Coastal Block, this siliciclastic succession shows interbedded rift-related Cambrian-Ordovician basaltic lenses (Pouclet et al., 2018). During the Devonian, a carbonatic platform developed in the WMM (Michard et al., 2010b and references therein), while sedimentation in the EMM continued to be mainly terrigenous (Hoepffner, 1987; Marhoumi et al., 1983). The metamorphism affecting the whole Paleozoic succession is generally of low- to very low-grade and the tectonic deformation seems to increase eastwards (Hoepffner et al., 2006).

The studied samples were collected in the Upper Devonian – Upper Carboniferous successions from different parts of the Moroccan Mesetas (Fig. 1C and D, Fig. 2, and Table 1 for coordinates). These successions are described in detail in the following subsections.

2.1. Ben Slimane area

The Lower-Middle Devonian succession of the Coastal Block and Central Zone of the WMM is mainly characterized by limestones deposited in a shelf (Zahraoui, 1991). Locally, the carbonate succession changes laterally to carbonatic olistoliths or turbiditic sandstones and shales, deposited in deeper environments.

At Middle Devonian time, the Coastal Block and Central Zone regions were affected by a general uplift, which culminated in the emersion of some areas and the subsidence of others (see subsection 2.2) during the Famennian. Thus, in the subsident Ben Slimane area (Fig. 1C), transgressive turbiditic sandstones, shales and deltaic quartzitic sandstones (Piqué, 1979, 1984; Zahraoui, 1991) directly overlay the Lower-Middle Devonian carbonatic sequence. The turbiditic sedimentation continued until the Tournaisian with local hiatus (Fig. 2; Zahraoui, 1991). A new subsiding phase started at Late Visean time (Izart, 1991) with the deposition of fossiliferous sandstones and shales with limestone intercalations (Destombe, 1987; Zahraoui, 1991).

The Triassic succession, characterized by red shales, conglomerates and basaltic lavas, unconformably overlays the Late Visean sediments (Fig. 2; Destombe, 1987).

2.2. Sidi Bettache area

The Sidi Bettache area (Fig. 1C) attests an allegedly pull-apart basin opened at Famennian-Tournaisian time (Piqué, 1979, 1984) in a regional contractive context (Fadli, 1990; Hoepffner, 1987; Piqué, 1979; Rolin et al., 1985). The opening of the basin triggered the deposition of turbiditic sequences dominated by quartzitic sandstones, conglomerates, and shales (Piqué et al., 1989), which transgressively overlie the Lower-Middle Devonian limestones (Fig. 2; Destombe, 1987. Locally, along the main faults bounding the Sidi Bettache basin, limestone olistoliths were deposited (Piqué et al., 1989), while gabbroic dikes and, in a lesser amount, dolerite lavas were emplaced (Fig. 2; Kharbouch, 1994; Kharbouch et al., 1989; Piqué, 1979).

Most of the Lower Visean succession, characterized by turbiditic deposits of sandstones and shales, was eroded during a period of subaerial emersion (Izart and Vieslet, 1988), with Middle-Upper Visean turbiditic sandstones, shales, and greywackes transgressively resting on the Tournaisian-lowermost Visean succession (Fig. 2; Bouabdelli, 1989; Izart, 1991; Termier et al., 1975; Verset, 1983, 1985). Nonetheless, a recent review of the micropaleontological content of the Visean succession suggests that the Lower-Middle Visean sediments are absent in the Sidi Bettache basin (Cózar et al., 2020).

The terrigenous sedimentation continued in the Serpukhovian-Middle Bashkirian (corresponding to the former Namurian) with the deposition of turbiditic shales, greywackes, and carbonatic sandstones (Beauchamp and Izart, 1987; Chakiri and Tahiri, 2000; Izart, 1991; Piqué, 1984; Zahraoui, 1991). The Middle Bashkirian-Kasimovian (corresponding to the former Westphalian) is characterized by the deposition of alternating conglomerates and fossiliferous black limestones deposited in a lacustrine environment (Cailleux et al., 2001; Piqué, 1984).

The Permian succession, characterized by red conglomerates, shales, and sandstones with intercalations of volcanic ashes and rhyolitic lavas (El Wartiti, 1994), unconformably overlays the Middle Bashkirian-

Fig. 1. A) Schematic map of NW Africa and Iberia showing the location of the northern Moroccan Variscides (rectangle); SPZ: South Portuguese Zone; OMZ: Ossa-Morena Zone; M: Mauritanides; CIZ: Central Iberian Zone; B) Geological map of the northern Moroccan Variscides (after Hoepffner et al., 2006; Michard et al., 2010b). RTFZ: Rabat-Tiflet Fault Zone; WMSZ: Western Meseta Shear Zone; SOFZ: Smaala-Oulmès Fault Zone; TBBFZ: Tazekka-Bsabis-Bekrit Fault Zone; TTFZ: Tizin'Test Fault Zone; SMFZ: South Meseta Fault Zone; SAFZ: South Atlas Fault Zone. C) Schematic geological map of part of the Western Moroccan Meseta (after Becker and El Hassani, 2020) with location of the studied samples. D) Schematic geological map of part of the Eastern Moroccan Meseta (after Muratet, 1988) with location of the studied samples.

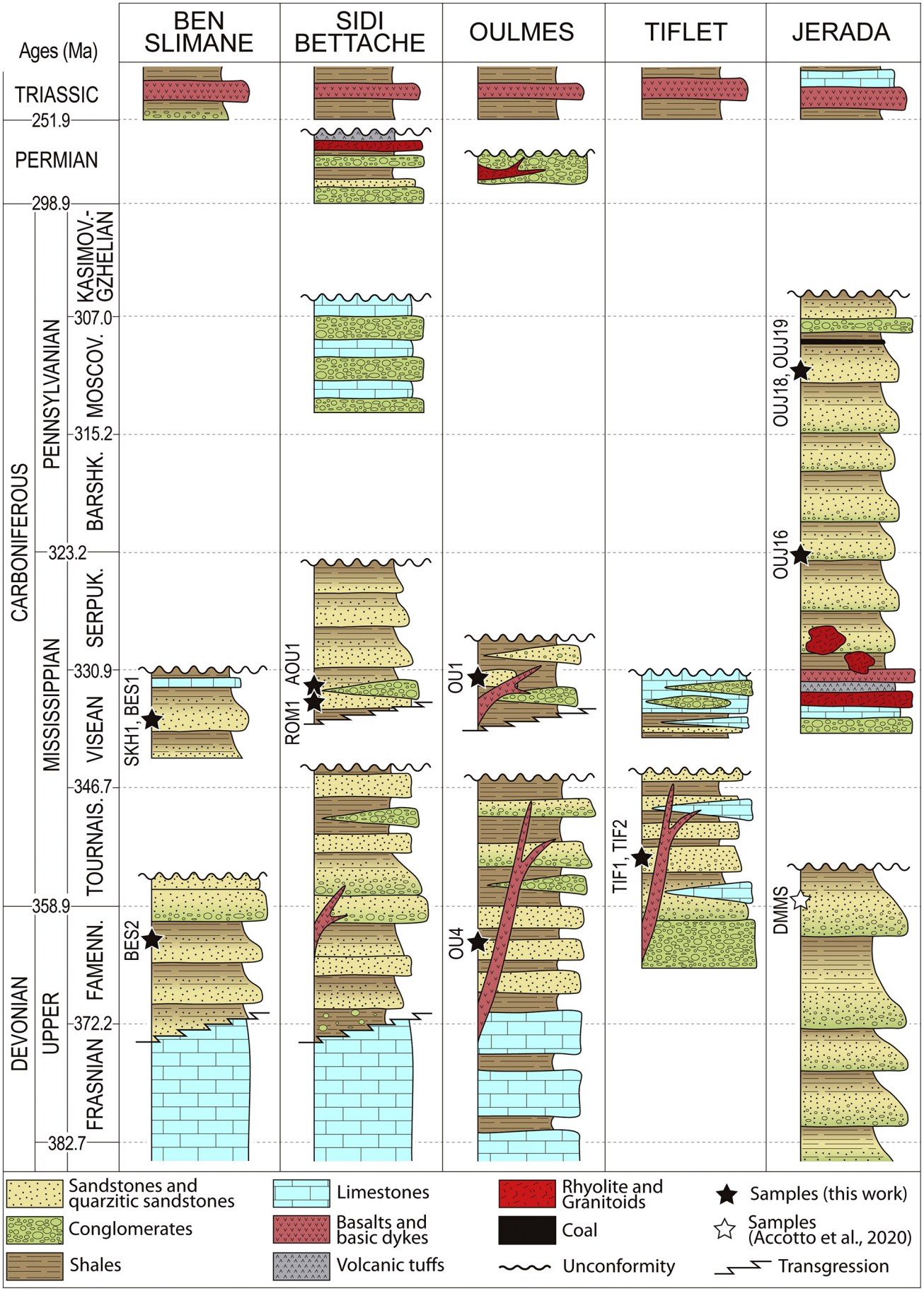
Ages (Ma)
BEN SLIMANE
SIDI BETTACHE
OULMES
TIFLET
JERADA
TRIASSIC
251.9
PERMIAN
298.9
CARBONIFEROUS
PENNSYLVANIAN
KASIMOV.-GZHELIAN
307.0
MOSCOV.
315.2
BARSHK.
323.2
MISSISSIPPIAN
SERPUK.
330.9
VISEAN
346.7
TOURNAIS.
358.9
DEVONIAN
UPPER
FAMENN.
372.2
FRASNIAN
382.7
SKH1, BES1
ROM1
AOU1
OU1
OUJ18, OUJ19
OUJ16
TIF1, TIF2
BES2
OU4
DMMS
Sandstones and quarzitic sandstones
Conglomerates
Shales
Limestones
Basalts and basic dykes
Volcanic tuffs
Rhyolite and Granitoids
Coal
Unconformity
Samples (this work)
Samples (Accotto et al., 2020)
Transgression

Kasimovian rocks (Fig. 2). Finally, Triassic red shales and basaltic lavas unconformably overlay the Permian and pre-Permian successions (El Touhami, 1993).

2.3. Oulmes area

The Oulmes area is part of a structural high separating the Sidi Bettache and Fourhal areas (Khouribga-Oulmes area in Fig. 1C). The Upper Devonian succession is characterized by alternation of fossiliferous nodular limestones and shales, dated at the Frasnian-Famennian (Kaiser et al., 2007), passing upward to Upper Famennian quartzitic sandstones (Fig. 2). During the Tournaisian, the deposition of shales was acompaigned by local olistoliths of Middle Devonian limestones and beds of turbiditic sandstones (Izart et al., 2001). The Upper Visean- Serpukhovian shales with lenses of sandstones directly rest on the Tournaisian succession and are unconformably overlain by Permian continental conglomerates (El Hassani et al., 2002; Izart et al., 2001). The entire Upper Devonian-Carboniferous succession is cross-cut by basic and acid dykes (Izart et al., 2001; Kharbouch, 1994; Kharbouch et al., 1985) and intruded by Late Carboniferous-Permian granitoids (Izart et al., 2001). The Triassic red shales and basaltic lavas unconformably overlie the Permian conglomerates.

2.4. Tiflet area

To the south of the RTFZ, the Upper Famennian-Upper Visean succession of the Bou Regreg corridor (Fig. 1C) unconformably overlies the Lower Devonian succession, the latter being characterized by black shales and black fossiliferous limestones of Lochkovian-Emsian age (Alberti, 1969; El Hassani, 1991). The Famennian period is characterized by deposition of conglomerates (Fig. 2) with Ordovician-Devonian clasts (Lecointre and Delepine, 1933), dated by stratigraphic correlation with similar conglomerates cropping out in the Rabat area containing interbedded arkoses and shales with Famennian fossil plants (El Hassani, 1991 and references therein). The sedimentation continued with sandstones and shales interbedded with sporadic lenses of limestones containing Tournaisian fauna (Fig. 2; Lecointre and Delepine, 1933). Upwards, a 400 m-thick succession of sandstones and shales with abundant limestone lenses was dated as Lower Visean (Izart and Vieslet, 1988; Lecointre and Delepine, 1933), although recent studies have re-dated it as Upper Visean based on a review of their foraminiferal content (Cózar et al., 2020). The entire Upper Devonian-Tournaisian succession is intruded by Permian basic dykes (Fig. 2; Cailleux et al., 1983; Kharbouch, 1994). The Upper Visean sequence, characterized by oolitic limestones with conglomeratic lenses, unconformably overlies the Tournaisian (—Early Visean?) succession (El Hassani, 1991).

In this area, there is no record of Middle-Upper Carboniferous rocks, and the Triassic red shales and basalts unconformably overlie the Upper Visean succession (El Hassani et al., 2002).

2.5. Jerada area

Unlike the WMM, where the Devonian period was characterized by a carbonatic platform that was progressively fragmented, the EMM (Fig. 1D) experienced more or less continuous sedimentation (e.g. Debdou and Mekkam inliers) with a Devonian-Tournaisian thick siliciclastic turbiditic succession of shales, greywackes, and sandstones (Fig. 2; Hoepffner, 1989), intensely deformed by a Tournaisian-Early Visean tectonic event induced by the collision between the northern margin of Gondwana and an Avalonian promontory (inferred as the eastern prolongation of the Sehoul Block; Accotto et al., 2020).

After this tectonic event, sedimentation resumed during the Late Visean with the deposition of basal conglomerates in relatively small and fragmented basins, local and subordinate carbonatic platform deposits, and a thick volcano-sedimentary sequence with rhyolites, andesites, and tuffs (Izart, 1991; Kharbouch et al., 1989; Médioni, 1979). The Serpukhovian-Middle Bashkirian succession in the Jerada area (Fig. 2) is characterized by shales and sandstones, (Chellai et al., 2011; Muratet, 1988), typical of deltaic environments (Izart, 1991). Deltaic sedimentation continued during the Middle Bashkirian-Kasimovian, but the environment became progressively more lacustrine, accompanied by deposition of fluvial conglomerates and coal levels (Fig. 2; Chellai et al., 2011).

After a Late Carboniferous Variscan tectonic event responsible for open ENE-WSW trending folds (e.g. Hoepffner, 1989; Horon, 1952), Triassic red shales, basalts, and limestones unconformably overlay the Paleozoic succession (Fig. 2; Muratet, 1988).

3. Samples and methods

This study is based on the U–Pb and Hf isotopic analysis of 12 samples collected in different areas of the Moroccan Mesetas (Figs. 1 and 2). The samples are listed in Table 1, together with their location, lithology, stratigraphic age, as well as the number and kind of analyses carried out.

In the Ben Slimane area (Fig. 1C), sample BES2 is a Famennian (Upper Devonian; Fig. 2) white quartzitic sandstone collected a few kilometers north of Ben Slimane. At the microscope scale, it is composed of more than 90% of quartz grains with diameters between ca. 0.25 and 0.1 mm, not particularly rounded. Rare interstitial phyllosilicates are present. Samples BES1 and SKH1 are Visean (Fig. 2) white quartzitic sandstones collected in Ben Slimane and along the coast, north of Ben Slimane. Both samples are characterized at the microscopic scale by more than 90% of angular quartz grains with diameters between ca. 0.2 and 0.1 mm. Interstitial phyllosilicates are very rare.

From the Visean succession of the Sidi Bettache area we collected two samples (Figs. 1C and 2). Sample ROM1 was sampled a few kilometers West of the city of Rommani. This sample is a reddish sandstone characterized by abundant quartz grains (about 75%) with very variable diameters from ca. 0.05 to 0.3 mm. Interstitial phyllosilicates and Fe-oxides are also frequent. Sample AOU1 was collected about 7 km SE of the city of Aïn El Aouda and it is a reddish Late Visean sandstone made up of ≈ 70% of fine-grained quartz (ca. 0.05 mm in diameter) and abundant phyllosilicates and Fe-oxides.

Sample OU4 was collected about 14 km North of the city of Oulmes (Fig. 1C). It is a quartzitic sandstone of Famennian age (Fig. 2) composed of ≈ 70% of quartz grains, mainly rounded and with a diameter between ca. 0.25 and 0.1 mm. Interstitial phyllosilicates and oxides are frequent. Sample OU1 was collected about 30 km SW of Meknes (Fig. 1C), along the road connecting this city with Oulmes. It is an Upper Visean (Fig. 2) sandy shale with a very heterogeneous texture characterized by zones with a fine-grained matrix (less than 0.03 mm); other portions of the sample are made up of ≈ 80% of angular quartz clasts of ca. 0.05 mm in diameter, together with frequent interstitial phyllosilicates and Fe-oxides.

The two samples from the Tiflet area, TIF1 and TIF2, were collected 2 km East of Tiflet, along the Tiflet river (Fig. 1C). They are Tournaisian sandstones (Fig. 2) characterized by medium-sized (ca. 0.2–0.05 mm) grains of quartz (ca.70%), and abundant phyllosilicates and Fe-oxides.

Fig. 2. Schematic comparison among stratigraphic columns of the Upper Devonian-Triassic successions in different parts of the Moroccan Mesetas: Ben Slimane area (Destombe, 1987; Piqué, 1984; Zahraoui, 1991), Sidi Bettache area (Beauchamp and Izart, 1987; Cailleux et al., 2001; Chakiri and Tahiri, 2000; Cózar et al., 2020; El Wartiti, 1994; Izart, 1991; Kharbouch, 1994; Piqué, 1984; Razin et al., 2001; Vidal, 1989), Oulmes area (El Hassani et al., 2002; Izart et al., 2001; Kaiser et al., 2007), Tiflet area (Cózar et al., 2020; El Hassani, 1991, 1987; Kharbouch, 1994), and Jerada area (El Hadi et al., 2006; Hoepffner, 1989; Horon, 1952; Médioni, 1979, 1977; Muratet, 1988). Not to scale.

Table 1
List of samples and analyses carried out; (*) number of analyses and number of concordant results (in bold).

Sample	IGSN (IEACC)	Location (UTM, NDAS83)			Lithology	Age	U-Pb geochronology		Hf isotope analyses
		Zone	Lat. (m N)	Long. (m E)			Method	Analyses (*)	
BEN SLIMANE AREA									
BES1	0009	29S	3,720,500	674,467	Quartzitic sandstone	Visean	LA-ICPMS	150/**120**	107
BES2	0010	29S	3,724,273	671,847	Quartzitic sandstone	Famennian	LA-ICPMS	180/**156**	–
SKH1	0011	29S	3,748,316	678,921	Quartzitic sandstone	Visean	SHRIMP LA-ICPMS	52/**41** 104/**95**	90
SIDI BETTACHE AREA									
ROM1	0012	29S	37,122,830	719,745	Sandstone	Visean	SHRIMP LA-ICPMS	52/**42** 114/**88**	–
AOU1	0013	29S	3,736,131	708,680	Sandstone	Visean	SIMS LA-ICPMS	28/**26** 84/**72**	–
OULMES AREA									
OU1	0014	30S	3,731,845	244,382	Sandy shale	Late Visean	LA-ICPMS	124/**104**	–
OU4	0015	29S	3,716,170	777,438	Quartzitic sandstone	Famennian	LA-ICPMS	150/**134**	–
TIFLET AREA									
TIF1	0016	29S	3,752,612	750,380	Sandstone	Tournaisian	LA-ICPMS	100/**73**	66
TIF2	0017	29S	3,752,611	750,354	Sandstone	Tournaisian	LA-ICPMS	120/**89**	88
JERADA AREA									
OUJ16	0018	30S	3,796,135	587,342	Sandstone	Serpukhovian-Mid. Bashkirian	LA-ICPMS	150/**128**	128
OUJ18	0019	30S	3,796,505	587,288	Sandstone	Mid. Bashkirian -Kasimovian	SIMS LA-ICPMS	70/**58** 50/**46**	46
OUJ19	0020	30S	3,796,474	587,262	Sandstone	Mid. Bashkirian -Kasimovian	LA-ICPMS	130/**120**	106

Samples OUJ16, OUJ18, and OUJ19 were collected about 10 km East of Jerada (Fig. 1D), in the southern flank of the Jerada synform. Sample OUJ16 is a Serpukhovian-Middle Bashkirian sandstone (Fig. 2) characterized by a very variable grain-size. The matrix is mainly composed of 70% of rounded quartz grains with diameters of ca. 0.05 mm, interstitial phyllosilicates, and oxides. The clasts represent about 30% of the sample, have diameters of 0.3–0.8 mm, and comprise variable lithologies (e.g. angular quartz grains, quartzitic sandstones, volcanic rocks, and foliated shales). Samples OUJ18 and OUJ19 were both collected from sandstone layers within the Middle Bashkirian-Kasimovian succession (Fig. 2), being OUJ18 stratigraphically younger than OUJ19. They are both composed of abundant (ca. 65–70%) more or less rounded quartz grains with diameters varying between 0.05 and 0.2 mm. Phyllosilicates and oxides are also frequent, together with scarce glauconite.

For each sample, 4–5 kg of rock were collected and processed at the University of Granada (Spain). The separation processing of the detrital zircon grains included mechanical smashing with jaw- and ring-crusher, sorting with sieving, manual panning, and handpicking. A Mira3 VP-FESEM instrument at the John de Laeter Centre (JdLC) of Curtin University (Perth, Australia), and a Carl Zeiss SIGMA HD VP Field Emission SEM at the School of GeoSciences of the University of Edinburgh (United Kingdom) were used to obtain cathodoluminescence (CL) images of the zircon grains. A selection of these CL images is presented in Appendix A. Most of the detrital zircon grains were analyzed using laser ablation inductively coupled plasma mass spectrometer (LA-ICPMS) at the JdLC GeoHistory Facility. Nevertheless, in some samples, the size of the zircon grains was very variable and sensitive high-resolution ion microprobe (SHRIMP) and secondary ion mass spectrometry (SIMS) analyses were performed to grant a statistically significant number of results in each sample (Vermeesch, 2004). SHRIMP measurements were carried out at the JdLC, while SIMS analyses were performed at the University of Edinburgh. A more detailed description of the analytical methods can be found in Appendix B.

All the raw U–Pb results are listed in Appendix C. Concordant (with a discordance level ≤ 10%) $^{206}Pb/^{238}U$ dates were used for grains with ages younger than 1.5 Ga; for older grains $^{207}Pb/^{206}Pb$ concordant dates were used, due to the significant increase in error on $^{206}Pb/^{238}U$ dates for >1.5 Ga zircon grains. Kernel Density Estimators (KDE) and histograms of the concordant dates were made using DensityPlotter 8.4 (Vermeesch, 2012) applying a KDE bandwidth of 25 Ma and histogram bin of 20 Ma. Mean ages of the detrital zircon populations were calculated applying the mixture modelling tool in DensityPlotter 8.4 (Vermeesch, 2012) to groups of dates considered statistically (i.e. peaks in the KDE plots) and geologically (i.e. ages of the main geological events) meaningful. The ranges of dates used to calculate the mean ages of each population are detailed in section 4 (Results). The youngest age populations were calculated by using a weighted mean and assessed by the mean square weighted deviation (MSWD) within the software Isoplot (Ludwig, 2009, 2003) and IsoplotR (Vermeesch, 2018). Errors of mean ages and weighted mean ages are expressed at 1σ level.

Hf isotope analyses were run on those samples characterized by determinant detrital zircon populations (Carboniferous, Devonian, and Mesoproterozoic) in order to discriminate juvenile mantle-derived from recycled crustal-derived primary magmatic sources. These analyses were carried out at the JdLC on samples BES1, SKH1, TIF1, TIF2, OUJ16, OUJ18, and OUJ19 (Table 1). The details of the analytical methods are described in Appendix B, while the results are listed in Appendix D. Errors are expressed at 2σ level.

4. Results

4.1. Ben Slimane area

One hundred and eighty LA-ICPMS analyses were performed on detrital zircon grains from Famennian sample BES2, yielding 156 concordant results. The KDE diagram in Fig. 3A shows an important Cryogenian-Ediacaran population with an Ediacaran mean age of 612.8 ± 0.6 Ma (age range: ca. 701–542 Ma, $n = 98$, 62.8% of the data). A second detrital zircon population yielded a Rhyacian mean

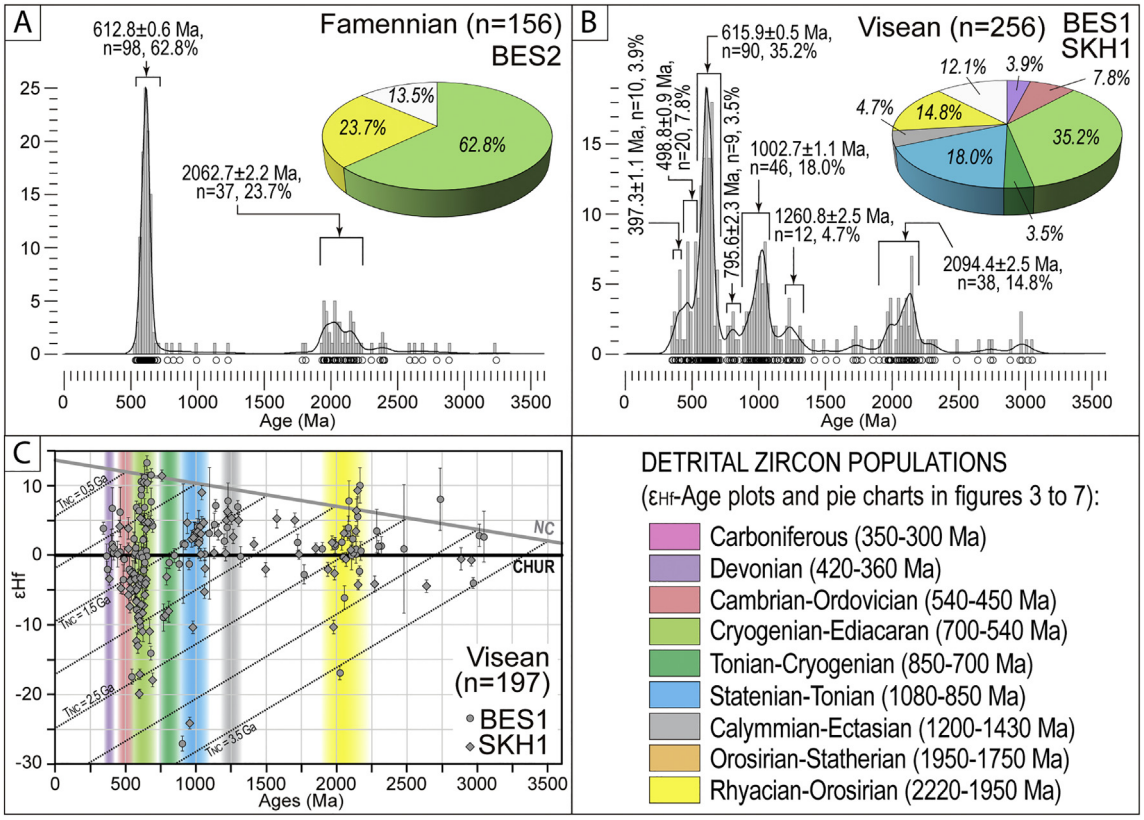

Fig. 3. U—Pb and Hf results in the Ben Slimane area. A and B) Kernel Density Estimates (KDE, black lines), histograms (grey bars), and pie-charts (colors correspond to the different ages of the detrital zircon populations as in legend; white represents scattered data) showing the detrital zircon age distribution of Famennian (A) and Visean (B) samples. C) ε_{Hf} values versus U—Pb ages for the Ben Slimane samples (BES1 and SKH1); CHUR: Chondritic Uniform Reservoir (Bouvier et al., 2008); NC: new crust (Dhuime et al., 2011); dotted lines indicate the TNC new crust ages of the bulk crust ($^{176}Lu/^{177}Hf = 0.015$). Colors indicate the different detrital zircon populations used in the text.

age of 2062.7 ± 2.2 Ma (ca. 2207–1932 Ma, $n = 37$, 23.7% of the data). A few scattered data have Archean-Rhyacian, Orosirian-Tonian, and Cambrian ages. The youngest detrital zircon population of this sample defines an Early Cambrian age (538.9 ± 3.0 Ma, MSWD = 1.38) and includes 4 dates.

The plot in Fig. 3B represents a combination of the results from the two statistically identical Visean samples (BES1 and SHK1). Two hundred and fifty-four LA-ICPMS analyses were carried out on the two samples, yielding 215 concordant results. On sample SHK1, 52 SHRIMP measurements were also run, giving 41 concordant dates. Furthermore, 197 Hf isotope analyses were performed on detrital zircon grains from both samples, the results of which are shown in Fig. 3C. The most outstanding feature of the resulting KDE/histogram plot (Fig. 3B) is a Cryogenian-Ediacaran peak, which includes 35.2% of the data ($n = 90$, ages from ca. 711 to 547 Ma) and yields an Ediacaran mean age of 615.9 ± 0.5 Ma. The ε_{Hf} values associated with this population ($n = 71$) show considerable variability (−19.8 and + 13.1). Second-order peaks gave Tonian-Stenian (1002.7 ± 1.1 Ma, ca. 1072–887 Ma, $n = 46$, 18% of the data) and Rhyacian-Orosirian (2094.4 ± 2.5 Ma, ca. 2224–1932 Ma, $n = 38$, 14.8% of the data) mean ages; both of these populations are characterized by mostly positive ε_{Hf} values, with a few scattered strongly negative ones (30 ε_{Hf} values between −26.9 and + 8.9 for the Tonian-Stenian population, and 28 data from −16.8 to +9.9 for the Rhyacian-Orosirian one). Minor detrital zircon populations are clustered at 1260.8 ± 2.5 Ma (ca. 1322–1206 Ma, $n = 12$, 4.7%; 11 ε_{Hf} values between −0.3 and + 7.8), 795.6 ± 2.3 Ma (ca. 852–764 Ma, n = 9, 3.5%; 7 ε_{Hf} values between −8.9 and + 11.3), 498.8 ± 0.9 Ma (ca. 538–450 Ma, $n = 20$, 7.8%; 14 ε_{Hf} values between −7.4 and + 6.1), and 397.3 ± 1.1 Ma (ca. 419–370 Ma, $n = 10$, 3.9%; 7 ε_{Hf} values between −3.4 and + 6.7). A few scattered dates have Archean-Rhyacian, Orosirian-Calymmian, and Stenian ages. The youngest detrital zircon populations of the Visean samples are Late Ediacaran (BES1: 578.3 ± 1.8 Ma, MSWD = 1.32, $n = 6$) and Early-

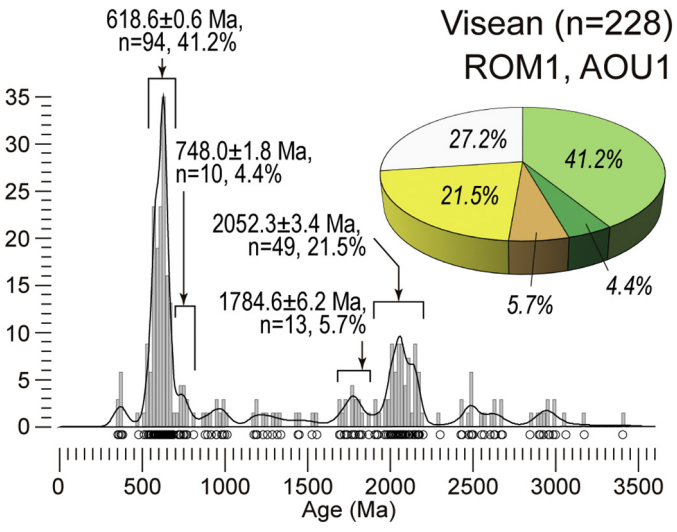

Fig. 4. Kernel Density Estimates (KDE, black lines), histograms (grey bars), and pie-charts (colors correspond to detrital zircon populations as indicated legend in Fig. 3; white represents scattered data) showing the detrital zircon age distribution of two Visean samples (ROM1 and AOU1) from the Sidi Bettache area.

Middle Ordovician (SKH1: 470.0 ± 2.3 Ma, MSWD = 1.30, n = 5); nonetheless, the youngest detrital zircon population of the combined two Visean samples is Early Devonian (409.7 ± 1.6 Ma, MSWD = 0.85, n = 5).

4.2. Sidi Bettache area

The results from the two Visean samples (ROM1 and AOU1) are represented in Fig. 4. One hundred and ninety-eight LA-ICPMS analyses were carried out, together with 52 SHRIMP and 28 SIMS measurements, which yielded a total of 228 concordant results. The most important detrital zircon population is Cryogenian-Ediacaran (ca. 686–543 Ma), which yielded an Ediacaran mean age of 618.6 ± 0.5 Ma (n = 94, 41.2% of the data). Another significant peak corresponds to the Rhyacian-Orosirian (ca. 2193–1902 Ma) population, with a mean age of 2052.3 ± 3.4 Ma (n = 49, 21.5% of the data). Minor detrital zircon populations gave Statherian (1784.6 ± 6.2 Ma, ca. 1824–1689 Ma, n = 13, 5.7% of the data) and Tonian (748.0 ± 1.8 Ma, ca. 808–716 Ma, n = 10, 4.4% of the data) mean ages. Scattered data have Paleoarchean-Rhyacian, Calymmian-Tonian, and Cambrian-Carboniferous ages. The youngest detrital zircon populations in these two samples are Late Ediacaran (AOU1: 583.7 ± 1.7 Ma, MSWD = 0.85, n = 6) and Late Devonian (ROM1: 373.6 ± 1.9 Ma, MSWD = 1.32, n = 4). If the two statistically identical samples are considered together as representative of the Visean succession in the area, the youngest detrital zircon population is Late Devonian (373.6 ± 1.9 Ma, MSWD = 1.32, n = 4).

4.3. Oulmes area

One hundred and fifty LA-ICPMS analyses were carried out on the detrital zircon grains from Famennian sample OU4, which yielded 134 concordant results (Fig. 5A). Three detrital zircon age populations can be identified in this sample, clustered at Cryogenian-Ediacaran (626.8 ± 0.5 Ma, ca. 717–549 Ma, n = 73, 54.5% of the data), Tonian-Stenian (1010.6 ± 1.7 Ma, ca. 1078–923 Ma, n = 13, 9.7% of the data) and Rhyacian-Orosirian (2049.4 ± 5.6 Ma, ca. 2133–2002 Ma, n = 14, 10.4% of the data). Furthermore, twelve dates yielded Cambrian-Devonian ages, although they do not define a peak in the KDE diagram. Scattered dates gave Archean-Siderian, Orosirian-Stenian, and Tonian ages. The youngest detrital zircon population includes 5 dates that define a Late Ediacaran age of 558.7 ± 1.7 Ma (MSWD = 1.04).

One hundred and twenty-four LA-ICMPS analyses were run on detrital zircon grains from the Visean sample OU1, yielding 104 concordant dates (Fig. 5B). The main detrital zircon age populations observed in this sample are Cryogenian-Ediacaran (ca. 685–543 Ma), with an Ediacaran mean age of 619.8 ± 0.4 Ma (n = 53, 51% of the data), and Rhyacian-Orosirian (ca. 2144–1940 Ma), with an Orosirian mean age of 2044.1 ± 1.8 Ma (n = 23, 22.1% of the data). A few scattered dates yielded Paleoarchean-Rhyacian, Statherian-Tonian, and Late Devonian ages. The youngest detrital zircon population gave a Late Ediacaran mean age of 561.9 ± 1.5 Ma and includes 4 dates (MSWD = 1.20).

4.4. Tiflet area

The KDE diagram and histogram in Fig. 6A show the results of the two Tournaisian samples (TIF1 and TIF2). Two hundred and twenty LA-ICPMS analyses were carried out on detrital zircon grains from those samples, 162 of which yielded concordant results. Together with the U–Pb analyses, 154 Hf isotope analyses were performed. The results are shown in Fig. 6B. Forty percent of the data are included in a Cryogenian-Ediacaran detrital zircon population (65 dates from ca. 713 Ma to ca. 544 Ma), which has an Ediacaran mean age of 614.5 ± 0.4 Ma and is characterized by a wide range of ε_{Hf} values (between −37.7 and + 11.9, n = 64). Secondary detrital zircon populations yielded Devonian (383.2 ± 0.6 Ma, ca. 415–361 Ma, n = 15, 9.3% of the data; 15 ε_{Hf} values from −10.6 to +1.9), Stenian-Tonian (1005.7 ± 1.3 Ma, ca. 1058–970 Ma, n = 13, 8% of the data; 11 ε_{Hf} values between −14.1 and + 7.0), and Orosirian-Statherian (1783.1 ± 3.9 Ma, ca. 1814–1747 Ma, n = 10, 6.2% of the data; 8 ε_{Hf} values between −17.0 and + 3.2) mean ages. Minor populations are clustered around 1357.2 ± 2.9 Ma (Calymmian, ca. 1433–1280 Ma, n = 8, 4.9% of the data; 8 ε_{Hf} values between −5.4 and + 7.7) and 2097.7 ± 4.0 Ma (Rhyacian, ca. 2177–1965 Ma, n = 11, 6.8% of the data; 11 ε_{Hf} values from −17.6 to +5.0). Scattered data have Mesoarchean-Rhyacian, Orosirian, Statherian-Calymmian, Ectasian-Stenian, Tonian, Cambrian-Ordovician, and Carboniferous ages. The youngest detrital zircon populations are Late Ediacaran in TIF1 (620.0 ± 1.5 Ma, MSWD = 1.4, n = 6) and Late Devonian in TIF2 (374.0 ± 1.5 Ma, MSWD = 0.88, n = 4). Combining both samples, the youngest detrital zircon population is Late Devonian and corresponds to the youngest detrital zircon population in TIF2.

4.5. Jerada area

One Serpukhovian-Middle Bashkirian (OUJ16) and two Middle Bashkirian-Kasimovian samples (OUJ18 and OUJ19) were collected in this area. The results are shown in Fig. 7A, where all the concordant data have been plotted together, being the three samples statistically identical and representative of the Middle Carboniferous succession in

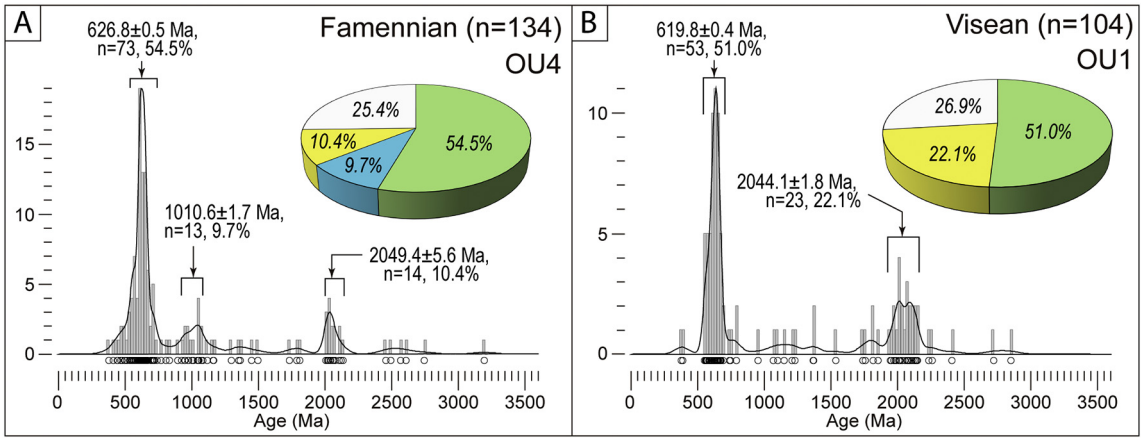

Fig. 5. Kernel Density Estimates (KDE, black lines), histograms (grey bars), and pie-charts (colors correspond to detrital zircon populations as in legend indicated Fig. 3; white represents scattered data) showing the detrital zircon age distribution of a Famennian (A; OU4) and a Visean (B; OU1) sample from the Oulmes area.

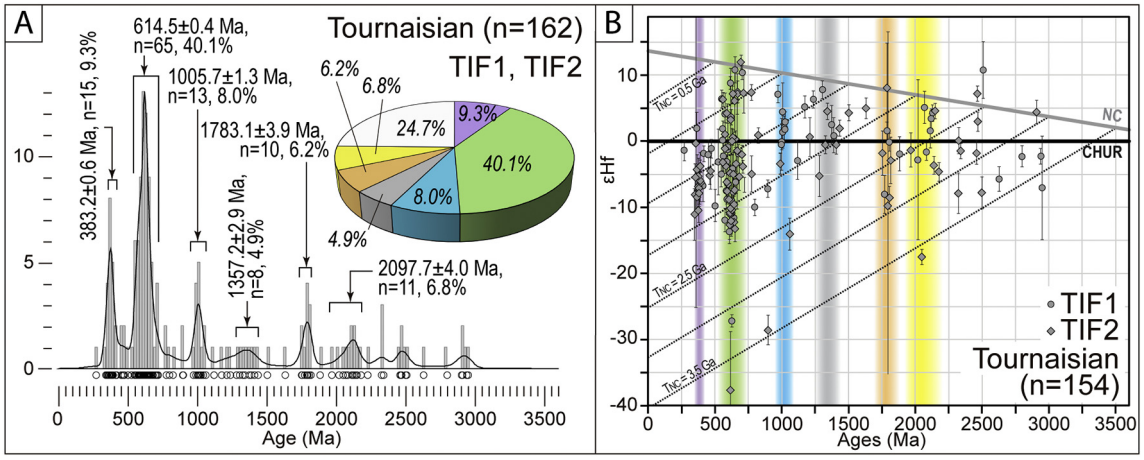

Fig. 6. U—Pb and Hf results in the Tiflet area. A) Kernel Density Estimates (KDE, black lines), histograms (grey bars), and pie-charts (colors correspond to detrital zircon populations as indicated legend in Fig. 3; white represents scattered data) showing the detrital zircon age distribution of two Tournaisian samples (TIF1 and TIF2). B) ε_{Hf} values versus U—Pb ages for samples TIF1 and TIF2; CHUR: Chondritic Uniform Reservoir (Bouvier et al., 2008); NC: new crust (Dhuime et al., 2011); dotted lines indicate the TNC new crust ages of the bulk crust ($^{176}Lu/^{177}Hf = 0.015$). Colors indicate the detrital zircon populations described in the text (see Fig. 3 for legend).

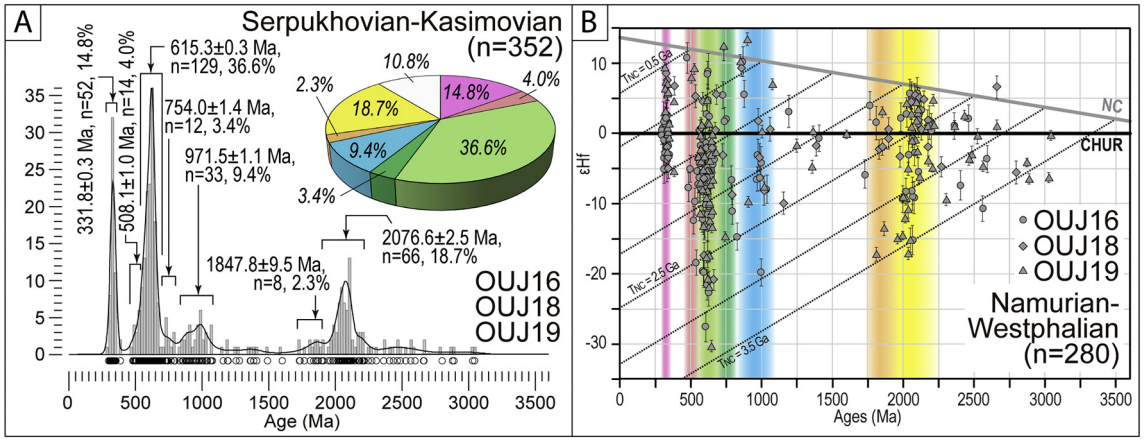

Fig. 7. U—Pb and Hf results in the Jerada area. A) Kernel Density Estimates (KDE, black lines), histograms (grey bars), and pie-charts (colors correspond to detrital zircon populations as in legend indicated Fig. 3; white represents scattered data) showing the detrital zircon age distribution of Serpukhovian-Middle Bashkirian (OUJ16) and Middle Bashkirian-Kasimovian (OUJ18 and OUJ19) samples. B) ε_{Hf} values versus U—Pb ages for samples OUJ16, OUJ18, and OUJ19; CHUR: Chondritic Uniform Reservoir (Bouvier et al., 2008); NC: new crust (Dhuime et al., 2011); dotted lines indicate the TNC new crust ages of the bulk crust ($^{176}Lu/^{177}Hf = 0.015$). Colors indicate the detrital zircon populations described in the text (see Fig. 3 for legend).

this area. Three hundred and thirty LA-ICMPS analyses were carried out, with 294 concordant results, 280 of which were then analyzed for Hf isotope signature (Fig. 7B). Due to the variable size of zircon grains in sample OUJ18, 70 additional SIMS analyses were run on this sample to reach a statistically representative number of data points; 58 of the SIMS analyses gave concordant dates. The most important detrital zircon age population in these samples is Cryogenian-Ediacaran, which yields a mean age of 615.3 ± 0.3 Ma (dates from ca. 685 to 543 Ma, $n = 129$; 36.6% of the data); one hundred and three of these zircon spots were analyzed for Hf isotopes and yielded ε_{Hf} values varying between −30.1 and + 9.0. Nineteen percent of the data ($n = 66$) are clustered at Rhyacian-Orosirian ages (ca. 2218–1900 Ma) with a mean age of 2076.6 ± 2.5 Ma and a considerable variability in ε_{Hf} values (−16.9 to +5.9, $n = 58$). Another important detrital zircon population yielded a Late Visean mean age (331.8 ± 0.3 Ma, dates from 351 to 297 Ma, $n = 52$, 14.8% of the data). The ε_{Hf} values of this Carboniferous population are variable between −4.8 and + 9.5 ($n = 44$). Minor populations gave Cambrian (508.1 ± 1.0 Ma, ca. 538–478 Ma, $n = 14$, 4% of the data; 8 ε_{Hf} values from −12.2 to +10.9), Late Tonian (754.0 ± 1.4 Ma, ca. 796–702 Ma, n = 12, 3.4% of the data; 8 ε_{Hf} values from −14.5 to +11.3), Early Tonian (971.5 ± 1.1 Ma, ca. 1077–851 Ma, $n = 33$, 9.4% of the data; 19 ε_{Hf} values between −19.7 and + 12.2), and Orosirian (1847.8.8 ± 9.5 Ma, ca. 1895–1811 Ma, n = 8, 2.3% of the data; 7 ε_{Hf} values between −17.0 and + 3.2) mean ages. Very scattered data yielded Mesoarchean-Rhyacian, Statherian-Stenian, Tonian, and Middle Devonian ages. The youngest detrital zircon populations in the three samples are Serpukhovian-Middle Bashkirian (OUJ16: 323.0 ± 1.5 Ma, MSWD = 1.4, n = 4; OUJ18: 322.0 ± 2.5 Ma, MSWD = 0.35, n = 4) and Visean (OUJ19: 339.3 ± 0.7 Ma, MSWD = 1.32, $n = 7$). Combining the three samples, the youngest detrital zircon population includes 6 dates and yields an Early Bashkirian mean age (316.6 ± 0.9 Ma, MSWD = 1.25).

To sum up, Cryogenian-Ediacaran and Rhyacian-Orosirian populations are always present in the studied Upper Devonian to Carboniferous samples, though at very different percentages. The Cryogenian-Ediacaran population encompasses 35–65% of the data, while the Rhyacian-Orosirian one represents 5–20% of the data. Taking into account all of the samples, up to seven minor detrital zircon populations can be defined: Orosirian-Statherian (ca. 1950–1750 Ma), Calymmian-Ectasian (ca. 1430–1200 Ma), Stenian-Tonian (ca.

1080–850 Ma), Tonian-Cryogenian (ca. 850–700 Ma), Cambrian-Ordovician (ca. 540–450 Ma), Devonian (ca. 420–360 Ma), and Carboniferous (ca. 350–300 Ma). The distribution of these populations in each area is summarized in Table 2.

5. Discussion

5.1. Maximum depositional ages

The youngest detrital zircon population in a sample is often used to define the maximum depositional age (MDA) of the rock (see Dickinson and Gehrels (2009) for methodology, and Sharman and Malkowski (2020) for discussion). This kind of data might be particularly useful to constrain the true depositional age (TDA) of the sediment, generally inferred either from the fossiliferous/palynological content or regional stratigraphic correlation. TDA can be coeval or younger than MDA (e.g. Sharman and Malkowski, 2020) depending on the geodynamic and geographic setting in which the sediment was deposited.

All of the studied samples have MDA spanning from Late Ediacaran (ca. 585 Ma) to Late Carboniferous (ca. 315 Ma), which are coherent with the TDA based on palynomorphs/paleontological studies and/or regional stratigraphic correlation (Destombe, 1987; El Hassani, 1991 and references therein; Horon, 1952; Izart, 1991 and references therein; Kaiser et al., 2007; Muratet, 1988; Vidal, 1989; Zahraoui, 1991 and references therein). When considering groups of samples with similar TDA (see section 4; Fig. 2), the Late Ediacaran youngest detrital zircon populations are replaced by Devonian to Late Carboniferous ones, thus suggesting that Devonian-Carboniferous magmatic rocks supplied detritus to all the Moroccan Mesetas, although in certain areas their impact is not noticeable in single samples. Our data show the necessity of exhaustive sampling and data density when trying to approximate MDA to TDA, especially in syn-orogenic settings, where high variability in the detrital zircon content is expected due to a combination of neoformed with mixed and recycled sources.

5.2. Provenance of pre-Devonian detrital zircon grains

Geochronological studies on detrital zircon grains from Late Ediacaran-Early Carboniferous samples of the Moroccan Variscides have been carried out by several authors (Abati et al., 2010, 2012; Accotto et al., 2019, 2020; Avigad et al., 2012; Ghienne et al., 2018; Letsch et al., 2018; Pérez-Cáceres et al., 2017) with the aim of finding out the main sources of sediments that fed the northern Gondwanan margin during the Paleozoic. All of these authors agreed that the main source area of sediments in the Moroccan Variscides is the West African Craton (WAC; Fig. 8), based on: (i) the recurrent presence of important Cryogenian-Ediacaran (ca. 0.6–0.75 Ga) and Paleoproterozoic (ca. 2.0 Ga) detrital zircon populations, which can be related to the Cadomian/Pan-African and Eburnean orogenic cycles, respectively (Nance et al., 2008 and references therein); and (ii) the absence of a significant Mesoproterozoic population, which is otherwise very common in areas affected by the Grenville orogeny (1.3–0.9 Ga; Ernst et al., 2008), such as Amazonia, Avalonia, and Baltica/Laurentia (Fig. 8), and in some European Variscan zones fed from the Arabian-Nubian shield and/or the Saharan Metacraton (e.g. Bea et al., 2010; Fernández-Suárez et al., 2014).

In terms of detrital zircon populations, the magmatic input of Cambrian-Ordovician Rheic Ocean rifting (Linnemann et al., 2008; Nance et al., 2012, 2010) in the Moroccan Variscides was scarce or negligible (Accotto et al., 2019, 2020; Ghienne et al., 2018; Letsch et al., 2018), except in a few, very localized areas (Letsch et al., 2018). In our samples, Cambrian-Ordovician zircon grains are rare (0–8% of the data). Cambrian mafic magmatic rocks are known in the Coastal Block (Pouclet et al., 2018), but they are restricted to volcanic focuses with limited spread. Therefore, we can infer that the Moroccan Variscides were only partially affected by the magmatism related to the Cambrian-Ordovician rifting, probably because of their more inland position in the Gondwana margin than other regions, such as the Ossa-Morena and Central Iberian Zones (Fig. 1A), where this kind of magmatism was ubiquitous and Cambrian-Ordovician detrital zircon

Table 2
Summary of the detrital zircon populations identified in each area, with approximate mean ages, percentage of occurrence, and, when available, range of ε_{Hf} values.

	BEN SLIMANE		SIDI BETTACHE	OULMES		TIFLET	JERADA
	FAMENNIAN	VISEAN	VISEAN	FAMENNIAN	VISEAN	TOURNAISIAN	SERPUKHOVIAN -BASHKIRIAN
CARBONIFEROUS ca. 350–300 Ma	–	–	–	–	–	–	ca. 330 Ma 14.8% ε_{Hf} − 4.8 / +9.5
DEVONIAN ca. 420–360 Ma	–	ca. 400 Ma 3.9% ε_{Hf} − 3.4 / +6.7	–	–	–	ca. 385 Ma 9.3% ε_{Hf} − 10.6 / +1.9	–
CAMBRIAN-ORDOVICIAN ca. 540–450 Ma	–	ca. 500 Ma 7.8% ε_{Hf} − 7.4 / +6.1	–	–	–	–	ca. 510 Ma 4.0% ε_{Hf} − 12.2 / +10.9
CRYOGENIAN-EDIACARAN ca. 700–540 Ma	ca. 615 Ma 62.8%	ca. 615 Ma 35.2% ε_{Hf} − 19.8 / +13.1	ca. 620 Ma 41.2%	ca. 630 Ma 54.5%	ca. 620 Ma 51.0%	ca. 615 Ma 40.1% ε_{Hf} − 37.7 / +11.9	ca. 615 Ma 36.6% ε_{Hf} − 30.1 / +9.0
TONIAN-CRYOGENIAN ca. 850–700 Ma	–	ca. 795 Ma 3.5% ε_{Hf} − 8.9 / +11.3	ca. 750 Ma 4.4%	–	–	–	ca. 750 Ma 3.4% ε_{Hf} − 14.5 / +11.3
STENIAN-TONIAN ca. 1080–850 Ma	–	ca. 1000 Ma 18.0% ε_{Hf} − 26.9 / +8.9	–	ca. 1010 Ma 9.7%	–	ca. 1005 Ma 8.0% ε_{Hf} − 14.1 / +7.0	ca. 970 Ma 9.4% ε_{Hf} − 19.7 / +12.2
CALYMMIAN-ECTASIAN ca. 1430–1200 Ma	–	ca. 1260 Ma 4.7% ε_{Hf} − 0.3 / +7.8	–	–	–	ca. 1355 Ma 4.9% ε_{Hf} − 5.4 / +7.7	–
OROSIRIAN-STATHERIAN ca. 1950–1750 Ma	–	–	ca. 1785 Ma 5.7%	–	–	ca. 1785 Ma 6.2% ε_{Hf} − 9.9 / +8.0	ca. 1850 Ma 2.3% ε_{Hf} − 17.0 / +3.2
RHYACIAN-OROSIRIAN ca. 2220–1950 Ma	ca. 2065 Ma 23.7%	ca. 2095 Ma 14.8% ε_{Hf} − 16.8 / +9.9	ca. 2055 Ma 21.5%	ca. 2050 Ma 10.4%	ca. 2045 Ma 22.1%	ca. 2100 Ma 6.8% ε_{Hf} − 17.6 / +5.0	ca. 2075 Ma 18.7% ε_{Hf} − 16.9 / +5.9

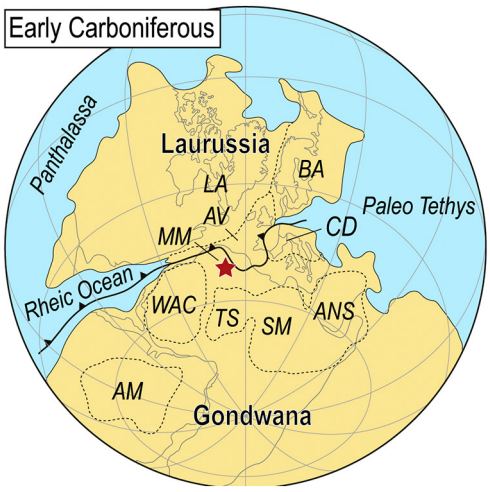

Ages (in Ga) of the main plutonic and volcanic events

WAC (West African Craton):	0.75 - 0.54 2.4 - 1.8 2.95 - 2.6 3.6 - 3.05	SM (Sahara Metacraton):	1.2 - 0.5 2.2 - 1.5 3.0 - 2.4
AV (Avalonia):	0.38 - 0.35 0.8 - 0.5 1.6 - 0.9 2.6 - 2.5	ANS (Arabian-Nubian Shield):	1.2 - 0.5 2.2 - 1.6 2.7 - 2.3 3.1 - 2.9
CD (Cadomia):	0.34 - 0.32 0.5 - 0.48 0.9 - 0.54 2.25 - 1.75	LA (Laurentia):	0.6 - 0.4 1.5 - 0.95 2.4 - 1.6 3.0 - 2.6
AM (Amazonia):	0.9 - 0.6 1.5 - 1.0 2.2 - 1.6 3.0 - 2.5	TS (Tuareg Shield):	0.9 - 0.5 2.2 - 1.6 3.0 - 2.5
MM (Moroccan Mesetas)		BA (Baltica):	0.65 - 0.45 2.2 - 0.95 3.25 - 2.4

Fig. 8. Paleogeographic reconstruction of Gondwana and Laurussia at Early Carboniferous time (after Murphy et al., 2016 and references therein; Nance et al., 2012 and references therein). Ages of the main magmatic events are from Abati et al. (2010), Bea et al. (2010), Cambeses et al. (2017) and references therein, Linnemann et al. (2011) and references therein, Marzoli et al. (2017) and references therein, Nance et al. (2008), Pereira et al. (2012, 2017), and Santos et al. (1987). The red star indicates the approximate location of the studied area.

grains are usually present in syn-orogenic rocks (Martínez Catalán et al., 2008; Pastor-Galán et al., 2013b; Pereira et al., 2020b).

A Stenian-Tonian (ca. 1.0 Ga) detrital zircon population is identified in the Moroccan Variscides (up to 30% of the data) although it is not present everywhere. This population was found in Ediacaran-Late Devonian samples from the Anti-Atlas (Avigad et al., 2012) and the Moroccan Mesetas (Accotto et al., 2019, 2020; Ghienne et al., 2018). To explain the occurrence of these ages, the source of which is unknown in the WAC (Fig. 8), a distal and probably intermittent NE African source (namely the Sahara Metacraton; Fig. 8) was invoked.

5.3. Source evolution during Late Devonian-Carboniferous time

In this study, we analyzed two Famennian samples (BES2 and OU4 in the Ben Slimane and Oulmes areas, respectively), which have the same detrital zircon populations as those described by other authors in the Moroccan Variscides (Abati et al., 2010, 2012; Accotto et al., 2019, 2020; Avigad et al., 2012; Letsch et al., 2018; Pérez-Cáceres et al., 2017), thus suggesting that in Late Devonian times, this part of the northern margin of Gondwana was still mostly fed by the WAC (Eburnean and Cadomian/Pan-African orogenies), together with some minor and distant NE African (ca. 1.0 Ga) sources recorded in the Oulmes area (Fig. 9A).

Slightly younger samples (Tournaisian) collected in the Tiflet area (TIF1 and TIF2) show a Devonian detrital zircon population, which could not have be supplied by the WAC. Very similar results were described by Accotto et al. (2020) in the Debdou-Mekkam area (EMM), and were interpreted as coming from a Devonian magmatic arc (Pereira et al., 2012), formed along the margin of an Avalonian terrane (e.g. Simancas et al., 2005) during the closure of the Rheic ocean and the first collisional stages between this terrane and northern Gondwana (Tournaisian-Early Visean; Accotto et al., 2020). This hypothesis is reinforced by the presence of Mesoproterozoic detrital zircon grains in these samples, which was also attributed to the approaching Avalonian block. Interestingly, the Tiflet area samples yielded a bimodal Mesoproterozoic detrital zircon population with peaks at ca. 1.0 and 1.35 Ga, which can be related to Grenvillian sources (e.g. Ernst et al., 2008). Because of the location of the Tiflet area (i.e. very close to the RTFZ separating the Moroccan Mesetas from the Caledonian Sehoul Block; Fig. 1C), we claim that Tournaisian sedimentation in this area was partially fed from this exotic terrane (Fig. 9B), which delivered zircon grains of Mesoproterozoic (Grenvillian orogeny) and Devonian (magmatic arc) ages; additionally, the WAC would have provided the Cryogenian-Ediacaran and Paleoproterozoic detrital zircon grains. The similarities between the Tournaisian samples from Tiflet and Debdou-Mekkam areas also extend to the Hf isotope data (Fig. 6B; Accotto et al., 2020). Actually, the Devonian ε_{Hf} range in the Tiflet samples (−10.6 to +1.9) is similar to that of sample MIM2 (−6 to 0) in the Debdou-Mekkam area. The new crustal ages (T_{NC}; Dhuime et al., 2011) of the Tiflet samples range from ca. 1.0 to 2.0 Ga, which suggests that these zircon grains formed from partial melting of Mesoproterozoic and Paleoproterozoic crust, supporting the hypothesis of Avalonian sources for the Devonian detrital zircon population. Furthermore, the Stenian-Tonian and Ectasian detrital zircon populations are characterized by mostly positive ε_{Hf} values (−5.4 to +7.7, with the exception of only one more negative value at −14.1), a range compatible with that seen in the Debdou-Mekkam area (ca. -5 to +5; Accotto et al., 2020) and some Avalonian terranes (ca. -5 to +7; Henderson et al., 2018 and references therein). These mostly positive data might indicate that the magmas in which the zircon grains formed were generated from Late Paleoproterozoic-Mesoproterozoic crust. Based on these similarities and assuming that the Debdou-Mekkam region was a fore-arc basin located at the front of the Avalonian promontory (Accotto et al., 2020), we can infer that the Tournaisian sediments in the Tiflet area might have been deposited in an analogous context but in a more lateral position with respect to the frontal promontory. Moreover, the Devonian detrital zircon population in the Tiflet samples (ca. 385 Ma) is slightly older than in the EMM (ca. 376 Ma), which might support an eastward migration of the Avalonian promontory, as well as the accompanying magmatic arc, in Late Devonian times.

After the initial collision between Gondwana and Avalonia (Late Tournaisian-Early Visean; Accotto et al., 2020), the detrital zircon spectra in younger syn-orogenic sediments are characterized by a mix of Gondwanan (WAC) and non-Gondwanan (Avalonian-Grenvillian) sources (Fig. 9C). This is particularly noticeable in a couple of samples from the Alborán Domain (Rif, Fig. 1B) published by Azdimousa et al. (2019), and in the Visean samples from the Ben Slimane area (BES1 and SKH1). All these samples, in fact, are characterized by a significant number of Mesoproterozoic dates. In particular, our samples include almost 5% of Ectasian (ca. 1.2–1.35 Ga) ages and, moreover, an Early Devonian (ca. 400 Ma) population that was not recorded in the Famennian sample (BES2). When looking at the Hf isotope signature, the ε_{Hf} values of the Devonian and Ectasian detrital zircon populations are very similar to those described in the Tiflet area. Therefore, we

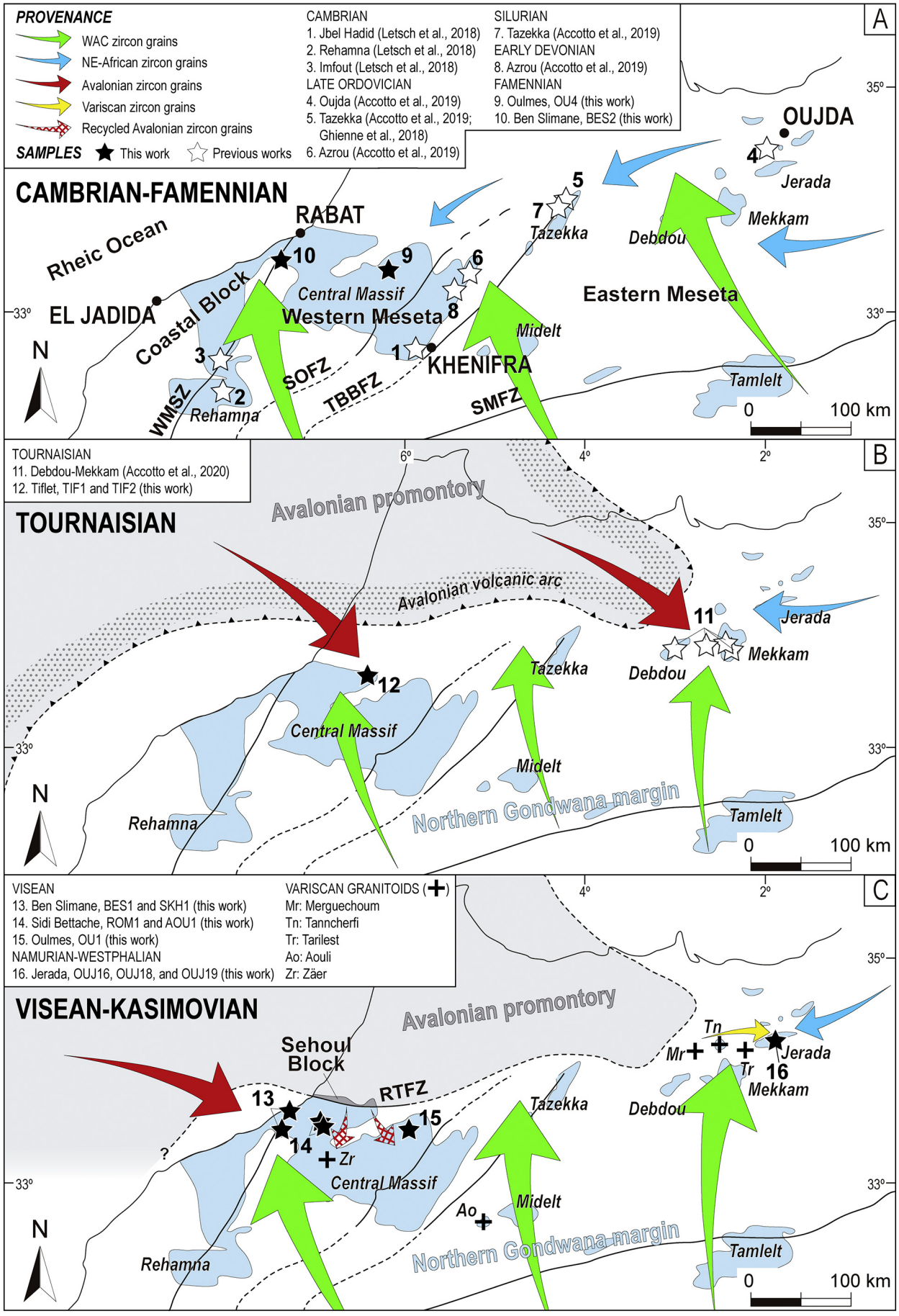
PROVENANCE
WAC zircon grains
NE-African zircon grains
Avalonian zircon grains
Variscan zircon grains
Recycled Avalonian zircon grains
SAMPLES This work Previous works
CAMBRIAN
1. Jbel Hadid (Letsch et al., 2018)
2. Rehamna (Letsch et al., 2018)
3. Imfout (Letsch et al., 2018)
LATE ORDOVICIAN
4. Oujda (Accotto et al., 2019)
5. Tazekka (Accotto et al., 2019; Ghienne et al., 2018)
6. Azrou (Accotto et al., 2019)
SILURIAN
7. Tazekka (Accotto et al., 2019)
EARLY DEVONIAN
8. Azrou (Accotto et al., 2019)
FAMENNIAN
9. Oulmes, OU4 (this work)
10. Ben Slimane, BES2 (this work)
A
CAMBRIAN-FAMENNIAN
RABAT
Rheic Ocean
EL JADIDA
Coastal Block
Central Massif
Western Meseta
Eastern Meseta
OUJDA
Jerada
Mekkam
Debdou
Tazekka
Midelt
KHENIFRA
Tamlelt
SOFZ
TBBFZ
SMFZ
WMSZ
Rehamna
N
0 100 km
TOURNAISIAN
11. Debdou-Mekkam (Accotto et al., 2020)
12. Tiflet, TIF1 and TIF2 (this work)
B
TOURNAISIAN
Avalonian promontory
Avalonian volcanic arc
Northern Gondwana margin
VISEAN
13. Ben Slimane, BES1 and SKH1 (this work)
14. Sidi Bettache, ROM1 and AOU1 (this work)
15. Oulmes, OU1 (this work)
NAMURIAN-WESTPHALIAN
16. Jerada, OUJ16, OUJ18, and OUJ19 (this work)
VARISCAN GRANITOIDS (+)
Mr: Merguechoum
Tn: Tanncherfi
Tr: Tarilest
Ao: Aouli
Zr: Zäer
C
VISEAN-KASIMOVIAN
Sehoul Block
RTFZ
Zr
Ao
Tn
Mr
Tr

conclude that these zircon grains might have been sourced from the erosion of the Avalonian promontory already accreted to the northern Gondwana margin or its lateral continuation offshore of the Atlantic Moroccan coast. In this regards, further south in the Oulad Dlim Massif (SW Morocco), the existence of non-Gondwana-derived rocks with a Silurian-Devonian (Caledonian) tectono-magmatic imprint (Bea et al., 2020; Gärtner et al., 2013) suggests that the Rheic Ocean suture might be located close to the Atlantic coastline.

In the Visean samples from the Sidi Bettache (ROM1, AOU1) and Oulmes areas (OU1), the influence of Avalonian sources seems to be minor as compared to the Ben Slimane area. In this regard, dates between ca. 1.6–1.05 Ga are scarce and very scattered in samples ROM1, AOU1 and OU1; combining the data of these three samples (Figs. 4B and 5), the Mesoproterozoic data represents ca. 6% of the dates, although the rather scattered distribution precludes the individualization of any detrital zircon population of that age. Therefore, the influence of the Avalonian promontory in the Sidi Bettache and Oulmes areas appears to be minor with respect to the Ben Slimane, Tiflet, and Debdou-Mekkam areas, probably due to the longer distance from the exotic block. Furthermore, since these Visean samples postdate the Eo-Variscan collision between the Avalonian promontory and Gondwana, part of the Mesoproterozoic zircon grains might have been recycled from previous syn-orogenic sediments of Tournaisian-Early Visean ages deposited in areas close to the Avalonian terrane (i.e. Tiflet area; Fig. 9C).

The Late Carboniferous samples from the Jerada area (OUJ16, OUJ18, and OUJ19) are characterized by detrital zircon spectra similar to older samples (i.e. Ordovician) from the Oujda EMM area (Accotto et al., 2019). Besides the Cryogenian-Ediacaran and Paleoproterozoic detrital zircon populations, the Oujda and Jerada samples are characterized by Stenian-Tonian dates clustered at ca. 0.95–0.97 Ga and representing 5–9% of the data. This similarity might suggest that the sources, at least in the eastern part of the EMM, did not change during the Ordovician-Carboniferous period. It is therefore plausible that the influence of the Avalonian promontory as a source of sediments only embraced the EMM to the Debdou-Mekkam area, while eastwards, the Oujda-Jerada region could have not received this input and represents a stable part of the northern Gondwana margin. Actually, the eastern part of the EMM (Beni Snassen, Oujda and Jerada areas) was not deformed during the initial collision between Avalonia and Gondwana (Accotto et al., 2020), and was principally fed by (primary or recycled) WAC sources during all of the Paleozoic and, to a lesser extent, by NE-African sources (e.g. Sahara Metacraton, Fig. 8).

The Late Carboniferous samples from the Jerada area are also characterized by ca. 15% of the data clustered in a Middle Carboniferous (ca. 330 Ma) detrital zircon population, with ε_{Hf} values ranging from −10 to +10, and T_{NC} from ca. 1.5 to 0.5 Ga. Variscan granitoids of Middle Carboniferous age are known in the EMM (e.g. Tarilest, Tanncherfi, and Merguechoum; El Hadi et al., 2006) and they probably represent the source of the detrital zircon grains with this age found in our samples. The crustal thickening originated by the collision between Avalonia and Gondwana (Accotto et al., 2020) probably induced an increase in the temperature within the Gondwanan crust, which, in turn, gave way to several middle Carboniferous igneous rocks, later exposed and partially eroded at Late Carboniferous times.

6. Conclusions

i) The systematic dating and Hf-isotopic characterization of Late Devonian-Late Carboniferous samples collected in several areas of the Moroccan Mesetas have allowed us to identify the influence of an allochthonous Avalonian promontory that approached and collided with the northern margin of Gondwana at Late Tournaisian-Early Visean time (Accotto et al., 2020). This Avalonian terrane is represented by the Sehoul Block, though it probably continues southwards offshore the Atlantic coastline.

ii) Before Late Devonian time, sediments in the Moroccan Variscides were sourced from the West African Craton, with a secondary and intermittent input from the distant Sahara Metacraton.

iii) The approaching and collision of the Avalonian promontory was recorded in Tournaisian samples from the Tiflet (this study) and Debdou-Mekkam (EMM; Accotto et al., 2020) areas, both characterized by a considerable number of Late Devonian (ca. 385–375 Ma) and Mesoproterozoic (ca. 1.6–1.0 Ga) zircon grains. The influence of this exotic terrane continued after its initial collision with Gondwana, delivering Devonian and Mesoproterozoic detrital zircon grains during the Visean in the adjacent areas to the Sehoul Block or its lateral prolongation offshore along the Moroccan Atlantic coastline.

iv) Among the Carboniferous samples analyzed, only those from the Ben Slimane are characterized by Mesoproterozoic and Devonian detrital zircon ages, while the samples from the Sidi Bettache, Oulmes, and Jerada areas did not recorded these dates or contain only a few (probably recycled) Mesoproterozoic grains.

v) The Late Carboniferous Jerada samples are characterized by a noteworthy Middle Carboniferous detrital zircon population sourced from syn-orogenic granites cropping out in the EMM and attesting the Early Variscan thickening and subsequent thermal maturation of the Gondwanan crust.

CRediT authorship contribution statement

Cristina Accotto: Conceptualization, Data curation, Formal analysis, Investigation, Methodology, Software, Visualization, Writing - original draft, Writing - review & editing. **David Martínez Poyatos**: Conceptualization, Funding acquisition, Investigation, Project administration, Supervision, Validation, Writing - original draft. **Antonio Azor**: Conceptualization, Investigation, Supervision, Validation, Writing - original draft. **Cristina Talavera**: Formal analysis, Methodology, Software. **Noreen Joyce Evans**: Formal analysis, Methodology, Software. **Antonio Jabaloy-Sánchez**: Conceptualization, Investigation. **Ali Azdimousa**: Resources. **Abdelfatah Tahiri**: Resources. **Hassan E.L. Hadi**: Resources.

Declaration of Competing Interest

The authors declare that they have no known competing financial interests or personal relationships that could have appeared to influence the work reported in this paper.

Acknowledgements

This study was founded by the Ministerio de Economía y Competitividad (MINECO) of Spain through the project PANGEATOR (CGL2015-71692) and the Pre-doctoral scholarship BES-2016-078168. The CL imaging was carried out in Curtin University's Microscopy & Microanalysis Facility, of which instrumentation has been partially funded by the University, State and Commonwealth Governments, and the Scanning Electron Microscope (SEM) Facility at the University of Edinburgh. Laboratory analyses on the detrital zircon grains were carried out on the SHRIMP II and GeoHistory Facility instruments of the JdLC,

Fig. 9. Evolutionary sketches showing the variation in detrital zircon sources in the Moroccan Mesetas. (A) Cambrian-Late Devonian, (B) Tournaisian, and (C) Visean-Kasimovian time.

supported by AuScope (auscope.org.au) and the Australian Government via the National Collaborative Research Infrastructure Strategy (NCRIS). The NPII multi-collector in the GeoHistory Facility was obtained via funding from the Australian Research Council LIEF program (LE150100013). The SIMS analyses were performed at the NERC Ion Microprobe Facility of the University of Edinburgh (UK). We are indebted to Mike Hall and Brad McDonald for their technical support on sample preparation and LA-ICPMS, respectively. The authors want to thank prof. R. Thomas Becker (University of Münster, Germany) for his insights into the Western Meseta stratigraphy. Reviews and comments by Dr. Gabriel Gutiérrez-Alonso, Prof. Dr. Ulf Linnemann, and Dr. Andrea Marzoli are warmly acknowledged.

Appendix A. Supplementary data

Supplementary material including the Appendix A, B, C, and D cited in the text might be found in Mendeley Datasets repository with the doi: 10.17632/x7zwsgzhnb.1 (https://data.mendeley.com/datasets/x7zwsgzhnb/draft?a=4c930b1c-4108-449f-abcf-f8cb1b7e3cb7). Supplementary data to this article can be found online at https://doi.org/10.1016/j.gr.2021.02.001.

References

Abati, J., Mohsine Aghzer, A., Gerdes, A., Ennih, N., 2010. Detrital zircon ages of Neoproterozoic sequences of the Moroccan Anti-Atlas belt. Precambrian Res. 181, 115–128. https://doi.org/10.1016/j.precamres.2010.05.018.

Abati, J., Aghzer, A.M., Gerdes, A., Ennih, N., 2012. Insights on the crustal evolution of the West African Craton from Hf isotopes in detrital zircons from the Anti-Atlas belt. Precambrian Res. 212–213, 263–274. https://doi.org/10.1016/j.precamres.2012.06.005.

Accotto, C., Martínez Poyatos, D.J., Azor, A., Talavera, C., Evans, N.J., Jabaloy-Sánchez, A., Azdimousa, A., Tahiri, A., El Hadi, H., 2019. Mixed and recycled detrital zircons in the Paleozoic rocks of the Eastern Moroccan Meseta: Paleogeographic inferences. Lithos 338–339, 73–86. https://doi.org/10.1016/j.lithos.2019.04.011.

Accotto, C., Martínez Poyatos, D., Azor, A., Jabaloy-Sánchez, A., Talavera, C., Evans, N.J., Azdimousa, A., 2020. Tectonic evolution of the EasternMoroccan Meseta: from Late Devonian forearc sedimentation to Early Carboniferous collision of an Avalonian promontory. Tectonics 39, 1–29. https://doi.org/10.1029/2019TC005976.

Alberti, G.K.B., 1969. Trilobiten des jüngeren Silurium sowie des Unter-und Mitteldevons. I. Mit Beitragen zur-Devon-Stratigraphie einiger Gebiete Marokko und Oberfranken, Abh Senckenb Naturforsch Ges.

Avigad, D., Gerdes, A., Morag, N., Bechstädt, T., 2012. Coupled U-Pb-Hf of detrital zircons of Cambrian sandstones from Morocco and Sardinia: Implications for provenance and Precambrian crustal evolution of North Africa. Gondwana Res. 21, 690–703. https://doi.org/10.1016/j.gr.2011.06.005.

Azdimousa, A., Jabaloy-Sánchez, A., Talavera, C., Asebriy, L., González-Lodeiro, F., Evans, N.J., 2019. Detrital zircon U-Pb ages in the Rif Belt (northern Morocco): Paleogeographic implications. Gondwana Res. 70, 133–150. https://doi.org/10.1016/j.gr.2018.12.008.

Bea, F., Montero, P., Talavera, C., Abu Anbar, M., Scarrow, J.H., Molina, J.F., Moreno, J.A., 2010. The palaeogeographic position of Central Iberia in Gondwana during the Ordovician: evidence from zircon chronology and Nd isotopes. Terra Nova 22, 341–346. https://doi.org/10.1111/j.1365-3121.2010.00957.x.

Bea, F., Montero, P., Haissen, F., Molina, J.F., Lodeiro, F.G., Mouttaqi, A., Kuiper, Y.D., Chaib, M., 2020. The Archean to Late-Paleozoic architecture of the Oulad Dlim Massif, the main Gondwanan indenter during the collision with Laurentia. Earth Sci. Rev. 103273. https://doi.org/10.1016/j.earscirev.2020.103273.

Beauchamp, J., Izart, A., 1987. Early Carboniferous basins of the Atlas-Meseta domain (Morocco): sedimentary model and geodynamic evolution. Geology 15, 797–800. https://doi.org/10.1130/0091-7613(1987)15<797:ECBOTA>2.0.CO;2.

Becker, R.T., El Hassani, A., 2020. Devonian to lower Carboniferous stratigraphy and facies of the Moroccan Meseta: implications for palaeogeography and structural Interpretation - a project outline. Hassan II Accademy of Science and Technology. Front. Sci. Eng. 10, 9–25.

Bouabdelli, M., 1989. Tectonique et sédimentation dans un bassin orogénique: le sillon viséen d'Azrou-Khenifra (Est du Massif Hercynien Central du Maroc). Ph.D. Thesis. Strasbourg, France, U.E.R. de Sciences de la vie et de la Terre, Institut de Géologie.

Bouvier, A., Vervoort, J.D., Patchett, P.J., 2008. The Lu–Hf and Sm–Nd isotopic composition of CHUR: Constraints from unequilibrated chondrites and implications for the bulk composition of terrestrial planets. Earth Planet. Sci. Lett. 273, 48–57. https://doi.org/10.1016/j.epsl.2008.06.010.

Cailleux, Y., Deloche, C., Gonord, H., Rolin, P., 1983. Les zones de cisaillement hercyniens en basse Meseta marocaine. Notes et Memoires du Service Géologique du Maroc 335, 199–209.

Cailleux, Y., Chevremont, P., Baudin, T., Razin, P., Chenakeb, M., Thieblemont, D., Hoepffner, C., Bensahal, A., Roger, J., Vaslet, D., 2001. Carte géologique du Maroc N°413: Ezzhiliga - Echelle 1/50.000. Royame du Maroc, Ministère l'Energie des Mines du Développement Durable.

Cambeses, A., Scarrow, J.H., Montero, P., Lázaro, C., Bea, F., 2017. Palaeogeography and crustal evolution of the Ossa–Morena Zone, Southwest Iberia, and the North Gondwana margin during the Cambro-Ordovician: a review of isotopic evidence. Int. Geol. Rev. 59, 94–130. https://doi.org/10.1080/00206814.2016.1219279.

Chakiri, S., Tahiri, A., 2000. La formation chaotique famenno-tournaisienne du Grou: témoin de la bordure orientale du bassin de Sidi Bettache (Meseta marocaine). Bull. l'Institut Sci. Rabat 22, 9–15.

Chellai, H., Essamoud, R., Rjimati, E.C., 2011. Le bassin houiller de Jerada (Chaîne des Horsts, Maroc oriental). In: Mouttaqi, A., Rjimati, E.C., Maacha, L., Michard, A., Soulaimani, A., Ibouh, H. (Eds.), Nouveaux Guides Géologiques et Miniers Du Maroc. Volume 9: Les Principales Mines Du Maroc. Notes et Memoires Du Service Géologique Du Maroc. 564, pp. 331–335.

Cózar, P., Vachard, D., Izart, A., Said, I., Somerville, I., Rodríguez, S., Coronado, I., El Houicha, M., Ouarhache, D., 2020. Lower-middle Viséan transgressive carbonates in Morocco: Palaeobiogeographic insights. J. Afr. Earth Sci. 168. https://doi.org/10.1016/j.jafrearsci.2020.103850.

Destombe, J., 1987. Carte géologique du Maroc N°350: Casablanca-Mohammedia - Echelle 1/100.000. Roy. du Maroc, Ministère l'Energie des Mines du Développement Durable.

Dhuime, B., Hawkesworth, C., Cawood, P., 2011. When continents formed. Science. 331, 154–155. https://doi.org/10.1126/science.1201245.

Dickinson, W.R., Gehrels, G.E., 2009. Use of U–Pb ages of detrital zircons to infer maximum depositional ages of strata: a test against a Colorado Plateau Mesozoic database. Earth Planet. Sci. Lett. 288, 115–125. https://doi.org/10.1016/j.epsl.2009.09.013.

El Hadi, H., Simancas, J.F., Tahiri, A., Gonzalez-Lodeiro, F., Azor, A., Martinez-Poyatos, D., 2006. Comparative review of the Variscan granitoids of Morocco and Iberia: proposal of a broad zonation. Geodin. Acta 19, 103–116. https://doi.org/10.3166/ga.19.103-116.

El Haibi, H., El Hadi, H., Tahiri, A., Martínez Poyatos, D., Gasquet, D., Pérez-Cáceres, I., González Lodeiro, F., Mehdioui, S., 2020. Geochronology and isotopic geochemistry of Ediacaran high-K calc-alkaline felsic volcanism: an example of a Moroccan perigondwanan (Avalonian?) remnant in the El Jadida horst (Mazagonia). J. Afr. Earth Sci. 163, 103669. https://doi.org/10.1016/j.jafrearsci.2019.103669.

El Hassani, A., 1987. Les structures calédono-hercyniennes dans la zone de Rabat-Tiflet (Meseta Marocaine septentrionale). Bull. l'Institut Sci. Rabat 11, 47–58.

El Hassani, A., 1991. La Zone de Rabat-Tiflet: bordure nord de la Chaîne Calédono-Hercynienne du Maroc. Bull. l'Institut Sci. Rabat 15, 1–34.

El Hassani, A., Tahiri, A., Chakiri, S., Zouine, E.M., Fedan, B., El Fellah, B., 2002. Carte géologique du Maroc N°398: Khemisset - Echelle 1/100.000. Royame du Maroc, Ministère l'Energie des Mines du Développement Durable.

El Houicha, M., Pereira, M.F., Jouhari, A., Gama, C., Ennih, N., Fekkak, A., Ezzouhairi, H., El Attari, A., Silva, J.B., 2018. Recycling of the Proterozoic crystalline basement in the Coastal Block (Moroccan Meseta): new insights for understanding the geodynamic evolution of the northern peri-Gondwanan realm. Precambrian Res. 306, 129–154. https://doi.org/10.1016/j.precamres.2017.12.039.

El Touhami, M., 1993. Le Trias évaporitique du bassin de Khémisset (Maroc Central): Géometrie des dépôts, Evolution sédimentaire et géochimie. Ph.D. Thesis. University Claude Bernard, Lyon, France.

El Wartiti, M., 1994. Le Permien. Bull. l'Institut Sci. Rabat 18, 84–92.

Ernst, R.E., Wingate, M.T.D., Buchan, K.L., Li, Z.X., 2008. Global record of 1600-700 Ma large Igneous Provinces (LIPs): Implications for the reconstruction of the proposed Nuna (Columbia) and Rodinia supercontinents. Precambrian Res. 160, 159–178. https://doi.org/10.1016/j.precamres.2007.04.019.

Fadli, D., 1990. Evolution sédimentaire et structurale des massifs de Mdakra et du Khatouat: deux segments hercyniens de la Meseta marocaine nord-occidentale. Ph. D. Thesis. Université Mohammed V, Rabat.

Fernández-Suárez, J., Gutiérrez-Alonso, G., Pastor-Galán, D., Hofmann, M., Murphy, J.B., Linnemann, U., 2014. The Ediacaran-early Cambrian detrital zircon record of NW Iberia: possible sources and paleogeographic constraints. 103, 1335–1357. https://doi.org/10.1007/s00531-013-0923-3.

Franke, W., Cocks, L.R.M., Torsvik, T.H., 2017. The Palaeozoic Variscan oceans revisited. Gondwana Res. 48, 257–284. https://doi.org/10.1016/j.gr.2017.03.005.

Gärtner, A., Villeneuve, M., Linnemann, U., El Archi, A., Bellon, H., 2013. An exotic terrane of Laurussian affinity in the Mauritanides and Souttoufides (Moroccan Sahara). Gondwana Res. 24, 687–699. https://doi.org/10.1016/j.gr.2012.12.019.

Ghienne, J.F., Benvenuti, A., El Houicha, M., Girard, F., Kali, E., Khoukhi, Y., Langbour, C., Magna, T., Míková, J., Moscariello, A., Schulmann, K., 2018. The impact of the end-Ordovician glaciation on sediment routing systems: a case study from the Meseta (northern Morocco). Gondwana Res. 63, 169–178. https://doi.org/10.1016/j.gr.2018.07.001.

Henderson, B.J., Collins, W.J., Brendan Murphy, J., Hand, M., 2018. A hafnium isotopic record of magmatic arcs and continental growth in the Iapetus Ocean: the contrasting evolution of Ganderia and the peri-Laurentian margin. Gondwana Res. 58, 141–160. https://doi.org/10.1016/j.gr.2018.02.015.

Hoepffner, C., 1987. La tectonique hercynienne dans l'Est du Maroc. Ph.D. Thesis. Université Louis Pasteur, Strasbourg.

Hoepffner, C., 1989. L'évolution structurale hercynienne de la Méséta marocain orientale. Essai de mise au point. Notes et Memoires du Service Géologique du Maroc 335, 229–237.

Hoepffner, C., Houari, M.R., Bouabdelli, M., 2006. Tectonics of the North African Variscides (Morocco, western Algeria): an outline. Compt. Rendus Geosci. 338, 25–40. https://doi.org/10.1016/j.crte.2005.11.003.

Horon, O., 1952. Contribution a l'étude du bassin de Djerada. Notes et Memoires du Protectorat de la Republique Française au Maroc 89, 180.

Izart, A., 1991. Les bassins carbonifères de la Méséta marocaine, étude sédimentologique et approche du contexte structural. Part de la tectonique et de l'eustatisme. Géologie Méditerranéenne 18, 61–72. https://doi.org/10.3406/geolm.1991.1452.
Izart, A., Vieslet, J.-L., 1988. Stratigraphie, sédimentologie et micropaléontologie du Famennien, Tournaisien et Viséen du bassin de Sidi-Bettache et de ses bordures (Meseta marocaine nord-occidentale). Notes et Mémoires du Service Géologique 334, 7–41.
Izart, A., Tahiri, A., El Boursoumi, A., Chevremont, P., 2001. Carte géologique du Maroc n° 411: Bouqachmir - echelle 1/50.000. Royame du Maroc, Ministère l'Energie des Mines du Développement Durable.
Kaiser, S.I., Becker, R.T., El Hassani, A., 2007. Middle to late Famennian successions at Ain Jemaa (Moroccan Meseta)—implications for regional correlation, event stratigraphy and synsedimentary tectonics of NW Gondwana. Geol. Soc. Lond. Spec. Publ. 278, 237–260. https://doi.org/10.1144/SP278.11.
Kharbouch, F., 1994. Le volcanisme dévono-dinantien du Massif central et de la Meseta orientale. Bull. l'Institut Sci. Rabat 18, 192–200.
Kharbouch, F., Juteau, T., Treuil, M., Joron, J.-L., Piqué, A., Hoepffner, C., 1985. Le volcanisme dinantien de la Meseta marocaine nord-occidentale et orientale. Caractères pétrographiques et géochimiques et implications géodynamiques. Sci. Géol. Bull. Mém. 38, 155–163.
Kharbouch, F., Juteau, T., Treuil, M., Joron, J.-L., Piqué, A., Hoepffner, C., 1989. Le complexe volcano-sédimentaire hercynien de la Méséta marocaine nord-occidentale et orientale: étude pétrographique, géochimique et signification géodynamique (Notes et Memoires du Service Géologique du Maroc).
Lecointre, G., Delepine, G., 1933. Etudes géologiques dans la région paléozoïque comprise entre Rabat et Tiflet. Notes et Memoires du Service Géologique du Maroc 28, 7–52.
Letsch, D., El Houicha, M., von Quadt, A., Winkler, W., 2018. A missing link in the peri-Gondwanan terrane collage: the Precambrian basement of the Moroccan Meseta and its lower Paleozoic cover. Can. J. Earth Sci. 55, 1–19. https://doi.org/10.1139/cjes-2017-0086.
Linnemann, U., Pereira, M.F., Jeffries, T.E., Drost, K., Gerdes, A., 2008. The Cadomian Orogeny and the opening of the Rheic Ocean: the diacrony of geotectonic processes constrained by LA-ICP-MS U-Pb zircon dating (Ossa-Morena and Saxo-Thuringian zones, Iberian and Bohemian Massifs). Tectonophysics 461, 21–43. https://doi.org/10.1016/j.tecto.2008.05.002.
Linnemann, U., Ouzegane, K., Drareni, A., Hofmann, M., Becker, S., Gärtner, A., Sagawe, A., 2011. Sands of West Gondwana: an archive of secular magmatism and plate interactions - a case study from the Cambro-Ordovician section of the Tassili Ouan Ahaggar (Algerian Sahara) using U-Pb-LA-ICP-MS detrital zircon ages. Lithos 123, 188–203. https://doi.org/10.1016/j.lithos.2011.01.010.
Ludwig, K.R., 2003. Isoplot 3.0. A geochronological toolkit for Microsoft Excel. Berkeley Geochron. 4. Center Special Publication, p. 70.
Ludwig, K.R., 2009. SQUID 2: A User's Manual (rev.12).
Marhoumi, M.R., Hoepffner, C., Doubinger, J., Rauscher, R., 1983. Données nouvelles sur l'histoire hercynienne de la Meseta orientale au Maroc: l'âge dévonien des schistes de Debdou et du Mekkam. Comptes Rendus l'Académie des Science de Paris 297, 69–72.
Martínez Catalán, J.R., Fernández-Suárez, J., Meireles, C., González Clavijo, E., Belousova, E., Saeed, A., 2008. U–Pb detrital zircon ages in synorogenic deposits of the NW Iberian Massif (Variscan belt): interplay of Devonian–Carboniferous sedimentation and thrust tectonics. J. Geol. Soc. Lond. 165, 687–698. https://doi.org/10.1144/0016-76492007-066.
Marzoli, A., Davies, J.H.F.L., Youbi, N., Merle, R., Dal Corso, J., Dunkley, D.J., Fioretti, A.M., Bellieni, G., Medina, F., Wotzlaw, J.F., McHone, G., Font, E., Bensalah, M.K., 2017. Proterozoic to Mesozoic evolution of North-West Africa and Peri-Gondwana microplates: detrital zircon ages from Morocco and Canada. Lithos 278–281, 229–239. https://doi.org/10.1016/j.lithos.2017.01.016.
Matte, P., 2001. The Variscan collage and orogeny (480-290 Ma) and the tectonic definition of the Armorica microplate: a review. Terra Nova 13, 122–128. https://doi.org/10.1046/j.1365-3121.2001.00327.x.
Médioni, R., 1977. Carte géologique du Maroc au 1/100.000. Feuille Debdou. Notice explicative. Notes et Memoires du Service Géologique du Maroc. 226 p. 63.
Médioni, R., 1979. Carte géologique du Maroc au 1/100.000. Feuille Hassiane Ed Diab. Notice explicative. Notes et Memoires du Service Géologique du Maroc. 227 p. 64.
Michard, A., Ouanaimi, H., Hoepffner, C., Soulaimani, A., Baidder, L., 2010a. Comment on Tectonic relationships of Southwest Iberia with the allochthons of Northwest Iberia and the Moroccan Variscides by J.F. Simancas et al. [C. R. Geoscience 341 (2009) 103-113]. Compt. Rendus Geosci. 342, 170–174. https://doi.org/10.1016/j.crte.2010.01.008.
Michard, A., Soulaimani, A., Hoepffner, C., Ouanaimi, H., Baidder, L., Rjimati, E.C., Saddiqi, O., 2010b. The South-Western Branch of the Variscan Belt: evidence from Morocco. Tectonophysics 492, 1–24. https://doi.org/10.1016/j.tecto.2010.05.021.
Muratet, B., 1988. Carte géologique du Maroc N°361: Aïn Bni Mathar - Echelle 1/100.000. Royame du Maroc, Ministère l'Energie des Mines du Développement Durable.
Murphy, J.B., Quesada, C., Gutiérrez-Alonso, G., Johnston, S.T., Weil, A., 2016. Reconciling competing models for the tectono-stratigraphic zonation of the Variscan orogen in Western Europe. Tectonophysics 681, 209–219. https://doi.org/10.1016/j.tecto.2016.01.006.
Nance, R.D., Murphy, J.B., Strachan, R.A., Keppie, J.D., Gutiérrez-Alonso, G., Fernández-Suárez, J., Quesada, C., Linnemann, U., D'lemos, R., Pisarevsky, S.A., 2008. Neoproterozoic-early Palaeozoic tectonostratigraphy and palaeogeography of the peri-Gondwanan terranes: Amazonian v. West African connections. Geol. Soc. Lond. Spec. Publ. 297, 345–383. https://doi.org/10.1144/SP297.17.
Nance, R.D., Gutiérrez-Alonso, G., Keppie, J.D., Linnemann, U., Murphy, J.B., Quesada, C., Strachan, R.A., Woodcock, N.H., 2010. Evolution of the Rheic Ocean. Gondwana Res. 17, 194–222. https://doi.org/10.1016/j.gr.2009.08.001.
Nance, R.D., Gutiérrez-Alonso, G., Keppie, J.D., Linnemann, U., Murphy, J.B., Quesada, C., Strachan, R.A., Woodcock, N.H., 2012. A brief history of the Rheic Ocean. Geosci. Front. 3, 125–135. https://doi.org/10.1016/j.gsf.2011.11.008.
Ouabid, M., Ouali, H., Garrido, C.J., Acosta-Vigil, A., Román-Alpiste, M.J., Dautria, J.M., Marchesi, C., Hidas, K., 2017. Neoproterozoic granitoids in the basement of the Moroccan Central Meseta: Correlation with the Anti-Atlas at the NW paleo-margin of Gondwana. Precambrian Res. 299, 34–57. https://doi.org/10.1016/j.precamres.2017.07.007.
Pastor-Galán, D., Gutiérrez-Alonso, G., Fernández-Suárez, J., Murphy, J.B., Nieto, F., 2013a. Tectonic evolution of NW Iberia during the Paleozoic inferred from the geochemical record of detrital rocks in the Cantabrian Zone. Lithos 182–183, 211–228. https://doi.org/10.1016/j.lithos.2013.09.007.
Pastor-Galán, D., Gutiérrez-Alonso, G., Murphy, J.B., Fernández-Suárez, J., Hofmann, M., Linnemann, U., 2013b. Provenance analysis of the Paleozoic sequences of the northern Gondwana margin in NW Iberia: Passive margin to Variscan collision and orocline development. Gondwana Res. 23, 1089–1103. https://doi.org/10.1016/j.gr.2012.06.015.
Pereira, M.F., Chichorro, M., Johnston, S.T., Gutiérrez-Alonso, G., Silva, J.B., Linnemann, U., Hofmann, M., Drost, K., 2012. The missing Rheic Ocean magmatic arcs: provenance analysis of late Paleozoic sedimentary clastic rocks of SW Iberia. Gondwana Res. 22, 882–891. https://doi.org/10.1016/j.gr.2012.03.010.
Pereira, M.F., El Houicha, M., Aghzer, A., Silva, J.B., Linnemann, U., Jouhari, A., 2014. New U-Pb zircon dating of late Neoproterozoic magmatism in Western Meseta (Morocco). Gondwana 15 - North meets South. 133 Doi:10.13140/2.1.2651.2641.
Pereira, M.F., El Houicha, M., Chichorro, M., Armstrong, R., Jouhari, A., El Attari, A., Ennih, N., Silva, J.B., 2015. Evidence of a Paleoproterozoic basement in the Moroccan Variscan Belt (Rehamna Massif, Western Meseta). Precambrian Res. 268, 61–73. https://doi.org/10.1016/j.precamres.2015.07.010.
Pereira, M.F., Gutíerrez-Alonso, G., Murphy, J.B., Drost, K., Gama, C., Silva, J.B., 2017. Birth and demise of the Rheic Ocean magmatic arc(s): combined U–Pb and Hf isotope analyses in detrital zircon from SW Iberia siliciclastic strata. Lithos 278–281, 383–399. https://doi.org/10.1016/j.lithos.2017.02.009.
Pereira, M.F., Gama, C., Dias da Silva, Í., Fuenlabrada, J.M., Silva, J.B., Medina, J., 2020a. Isotope geochemistry evidence for Laurussian-type sources of South Portuguese Zone Carboniferous turbidites (Variscan Orogeny). Geological Society of London https://doi.org/10.1144/SP503-2019-163 Special Publication SP503–2019–163.
Pereira, M.F., Gama, C., Dias da Silva, Í., Silva, J., Hofmann, M., Linnemann, U., Gärtner, A., 2020b. Chronostratigraphic framework and provenance of the Ossa-Morena Zone Carboniferous basins (SW Iberia). Solid Earth Discuss., 1–34 https://doi.org/10.5194/se-2020-26.
Pérez-Cáceres, I., Martínez Poyatos, D., Simancas, J.F., Azor, A., 2017. Testing the Avalonian affinity of the South Portuguese Zone and the Neoproterozoic evolution of SW Iberia through detrital zircon populations. Gondwana Res. 42, 177–192. https://doi.org/10.1016/j.gr.2016.10.010.
Piqué, A., 1979. Évolution structurale d'un segment de la chaîne hercynienne: la Meseta marocaine nord-occidentale. Ph.D. Thesis. Université de Strasbourg, France.
Piqué, A., 1984. Faciès sédimentaire et évolution d'un bassin: le Bassin dévono-dinantien de Sidi-Bettache (Maroc nord-occidental). Bull. l'Institut Sci. Rabat 6, 1015–1023.
Piqué, A., Cailleux, Y., Hoepffner, C., 1989. Plates-formes épicontinentales et sillons des flyschs au Paléozoïque dans la Méséta marocaine. Un domain sédimentaire à la marge du craton saharien. Notes et Memoires du Service Géologique du Maroc.
Pouclet, A., El Hadi, H., Álvaro, J.J., Bardintzeff, J.-M., Benharref, M., Fekkak, A., 2018. Review of the Cambrian volcanic activity in Morocco: geochemical fingerprints and geotectonic implications for the rifting of West Gondwana. Int. J. Earth Sci. 107, 2101–2123. https://doi.org/10.1007/s00531-018-1590-1.
Razin, P., Janjou, D., Baudin, T., Bensahal, A., Hoepffner, C., Chenakeb, M., Cailleux, Y., 2001. Carte géologique du Maroc N°412: Sidi Matla' Ech Chams - Echelle 1/50.000. Roy. du Maroc, Ministère l'Energie des Mines du Développement Durable.
Rolin, P., Cailleux, Y., Deloche, C., Gonord, H., 1985. Décrochements fini-dévoniens et ouverture de bassins de type pull-apart. Deux examples comparés: les bassins de Sidi Bettache (Maroc septentrional) et de Chateaulin (Bretagne occidentale, France). Géologie Africaine, Colloque, Congrès National Des Sociétés Savantes. 110, pp. 67–77.
Santos, J.F.H.P., Mata, J., Goncalves, F., Munha, J., 1987. Contribução para o conhecimento geológico-petrológico da região de Santa Susana: O complexo vulcano-sedimentar da Toca da Moura. Comunicacões dos Servicos Geológicos de Portugal 73, 29–48.
Sharman, G.R., Malkowski, M.A., 2020. Needles in a haystack: Detrital zircon U Pb ages and the maximum depositional age of modern global sediment. Earth Sci. Rev. 203, 103–109. https://doi.org/10.1016/j.earscirev.2020.103109.
Simancas, J.F., Tahiri, A., Azor, A., Lodeiro, F.G., Martínez Poyatos, D.J., El Hadi, H., 2005. The tectonic frame of the Variscan–Alleghanian orogen in Southern Europe and Northern Africa. Tectonophysics 398, 181–198. https://doi.org/10.1016/j.tecto.2005.02.006.
Simancas, J.F., Azor, A., Martínez-Poyatos, D., Tahiri, A., El Hadi, H., González-Lodeiro, F., Pérez-Estaún, A., Carbonell, R., 2009. Tectonic relationships of Southwest Iberia with the allochthons of Northwest Iberia and the Moroccan Variscides. Compt. Rendus Geosci. 341, 103–113. https://doi.org/10.1016/j.crte.2008.11.003.
Simancas, J.F., Azor, A., Martínez-Poyatos, D., Tahiri, A., El Hadi, H., González-Lodeiro, F., Pérez-Estaún, A., Carbonell, R., 2010. Reply to the comment by Michard et al. on "Tectonic relationships of Southwest Iberia with the allochthons of Northwest Iberia and the Moroccan Variscides.". Compt. Rendus Geosci. 342, 175–177. https://doi.org/10.1016/j.crte.2010.01.007.
Tahiri, A., Montero, P., El Hadi, H., Martínez Poyatos, D., Azor, A., Bea, F., Simancas, J.F., González Lodeiro, F., 2010. Geochronological data on the Rabat-Tiflet granitoids: their bearing on the tectonics of the Moroccan Variscides. J. Afr. Earth Sci. 57, 1–13. https://doi.org/10.1016/j.jafrearsci.2009.07.005.

Termier, G., Termier, H., Vachard, D., 1975. Recherches micropaléontologiques dans le Paléozoîque supérieur du Maroc central. Cah. Micropaleontol. 4, 1–90.
Vermeesch, P., 2004. How many grains are needed for a provenance study? Earth Planet. Sci. Lett. 224, 441–451. https://doi.org/10.1016/j.epsl.2004.05.037.
Vermeesch, P., 2012. On the visualisation of detrital age distributions. Chem. Geol. 312–313, 190–194. https://doi.org/10.1016/j.chemgeo.2012.04.021.
Vermeesch, P., 2018. IsoplotR: a free and open toolbox for geochronology. Geosci. Front. https://doi.org/10.1016/j.gsf.2018.04.001.
Verset, Y., 1983. Geotraverse du Maroc hercynien (Zone Nord), Stratigraphie et aperçus tectoniques. Journées 4 et 6 de l'excursion B1. Livret Guid. l'excursion B1.
Verset, Y., 1985. Carte géologique du Maroc au 1/100 000, feuille Quasbat-Tadla et Mémoire explicatif de la carte géologique (Notes Mémoires du Service Géologique du Maroc).
Vidal, J.C., 1989. Carte géologique du Maroc N°353: Rommani - Echelle 1/100.000. Royame du Maroc, Ministère l'Energie des Mines du Développement Durable.
Zahraoui, M., 1991. La plate-forme carbonatée dèvonienne du Maroc occidentale et sa dislocation hercynienne. Ph.D. Thesis. UBO, Brest, France.